

DRAFT

Electron Target Facility at Fermilab
and a Lepton-Quark Structure Experiment
The Nevis Laboratories Group *

Columbia University

May 1980

- I. Introduction
- II. Physics Objectives of Electron-Proton Studies
- III. The Lepton-Quark Experiment
- IV. The Electron Target and Interaction Region
- V. Cost Estimates and Schedules
- VI. Study of Running Eight Weeks in 1984
- VII. Appendix I: Calculation of Rates
Appendix II: Quark Distribution Functions
Appendix III: Fragmentation of Quark Jet
References
Figure Captions and Figures
- VIII. Addendums from the Workshop on e-p, May 3-4, 1980
 - A. Remarks by T. D. Lee
 - B. Theoretical Issues in e-p: C. H. Llewellyn Smith
 - C. e-p at Fermilab: T. Collins

* Proposal prepared by M. Atiya, W. Lee, T. O'Halloran,
H. Paar, F. Sciulli, R. Seto, R. R. Wilson, J. Wiss .

I. Introduction

In anticipation of a program of important experiments on the interaction at high energy of electrons and protons, we are proposing here the construction of an electron target facility at Fermilab and we will describe a specific experiment on the lepton-quark interaction that we would propose to Fermilab to be done at that facility. The facility might come into operation in 1984 at a cost of approximately \$20 million, the experiment might cost about \$10 million, so we are talking about an expenditure of roughly \$10 million per year for three years, and then normal operating costs. Even this first experiment should yield enough events to be able to measure an internal structure of the lepton or quark if it is greater than a five times 10^{-17} cm. It would also be sensitive to the existence of single or of multiple intermediate bosons up to a mass of about 300 GeV.

The electron target we are proposing is a 10 GeV electron storage ring (extendable to 15 GeV) to be added to the Tevatron at Fermilab so that c.m. energies up to 0.2 TeV and Q^2 values up to many thousands of GeV^2 can be explored. We anticipate the use of Columbia's Nevis Laboratories to whatever degree is necessary and desirable in the design and construction of the circulating electron target and of the detector. Of course, the characteristics and placement of the electron ring and of the interaction region must be the responsibility of Fermilab just as the civil construction must be either made

by them or under their direction. However, we stand ready to help on these problems to the extent that is welcome and useful. We are also aware of the magnitude of the effort required and are eager to join forces with others to realize the facility and to share in making experiments therein. The intensity of general interest in an ep facility was indicated by the attendance of 125 physicists at the "ep Workshop" held May 3 and 4 (a Sunday yet!), 1980 at Columbia University. Canadian physicists have also expressed a strong interest.

It is remarkable that electron-proton collisions, which are one of the most effective procedures for investigating the inner structure of matter, have been neglected in the press to realize lepton-lepton collisions on the one hand, and nucleon-nucleon collisions on the other; the lepton collisions because of the simplicity of the experiments, the nucleon collisions because of the tremendous energy available. But electron-proton collisions can also yield a wealth of information, information that is generally complementary to that given by the other collisions. For example, studies of neutral and charged current interactions can be extended to large momentum transfers, as in the lepton-quark experiment described here, intermediate bosons should produce large effects for masses up to about 350 GeV, polarized electron beams may reveal right-handed charge current at large Q^2 , new heavy objects may be observed, and perhaps most

importantly, the exploration of the inner structure of quarks or of leptons can be started.

If facilities for bringing electron beams into collision with proton beams are not yet being constructed, it is not for lack of study. Indeed extensive workshops have occurred at Fermilab for the Tevatron,¹ at Brookhaven for ISABELLE,² at CERN for the SPS,³ at DESY for Petra,⁴ and at KEK for Tristan.⁵ All of the investigations have been made in depth but the recent study for the HERA* project at DESY is the most definitive. Thus, the physics of electron-proton collisions has been well considered and the problem of preparing an electron target has also been looked into rather thoroughly. What we are proposing here is what must be done specifically in the United States in order to realize experiments with electron-proton colliding beams.

In these days when the appetites of meritorious projects already underway can easily absorb all the funds available, and that is why ep projects have not been started earlier, it may not seem an auspicious time to suggest yet a new project. But those projects already funded will be completed before long so that new undertakings should be considered now. What must be especially emphasized here is that very modest funding for electron-proton experiments can produce knowledge which will be competitive with that which will result from the more expensive projects. It is for this reason that we describe

* HERA is the acronym for a project for 30 GeV electrons on 820 GeV protons at a cost of about 600 million DM. It has not yet been approved for construction but if approved it might come into operation toward the end of the 1980's.

these experiments under the rubric of "electron target" in order to emphasize the modesty of the costs of the program.

When we confine ourselves to the possibilities of experiments which can be done in the United States, we can either bring electron beams to proton accelerators or proton beams to electron accelerators. This means building electron beams at Fermilab or at ISABELLE, or constructing proton beams at Cornell or SLAC, or, more expensively, constructing both electron and proton beams in a facility dedicated to ep experiments. The investment at Fermilab and at Brookhaven in proton accelerators would appear to make it almost prohibitive to duplicate such facilities elsewhere, hence we consider here only the first alternative of bringing the more modest electron ring to a proton establishment. For the sake of high energy, of timeliness, and of specificity, we will here consider a facility only at Fermilab. Fermilab has the additional attraction that 5 TeV protons may eventually be available there. It has also the potential of producing electrons with energies up to 50 GeV, which would allow for a sustained program of ep experiments which could eventually culminate in c.m. energies of 1 TeV, well beyond the unitarity limit.

In what follows, we will briefly discuss the importance of the physics, and will describe in detail the detector and the specific experiment to be made with it on the lepton-quark

interaction. A general design of the circulating ring and of the interaction region will be presented. Finally, we will give the results of a study made for the proposed experiment if it were to run for a total duration of 8-16 weeks for four consecutive years starting in 1984.

II. Physics Objectives of Electron-Proton Studies

The proposed electron target facility opens up a new kinematical range, heretofore inaccessible to fixed target electron, muon and neutrino experiments. The capabilities of this new facility cover a wide range of fundamentally interesting physics. Among the topics to be studied are:

1) Study of the structure of the proton, the quark and the electron.

2) Study of neutral current effects. With the kinematic region available, the strength of the γ and Z amplitudes are comparable. The availability of left and right handed circularly polarized beams for both electron and positron will make it possible to study the details of the weak and electromagnetic interaction.

3) The measurement of the propagator effect and hence deduce the mass of the W and Z mesons.

4) Search for right handed charge currents.

5) Tests of time reversal invariance.

6) The production of new flavored quarks.

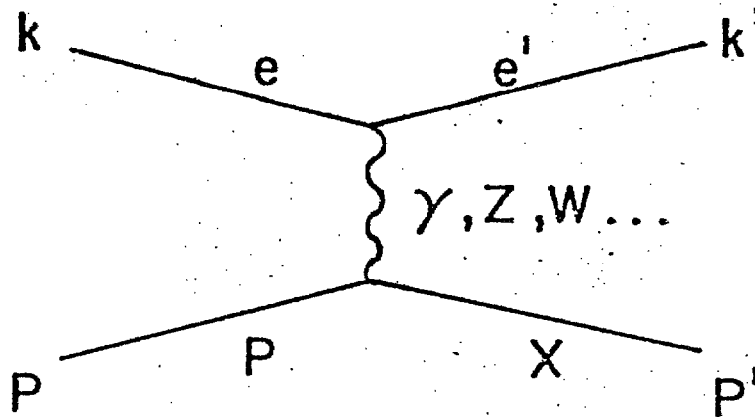
7) Photoproduction.

8) Hunt for new and exotic particles.

A. Kinematics

We describe below the notation we will use in this report.

Consider the reaction



$$s = (k+p)^2 = 4E_e E_p + m_p^2$$

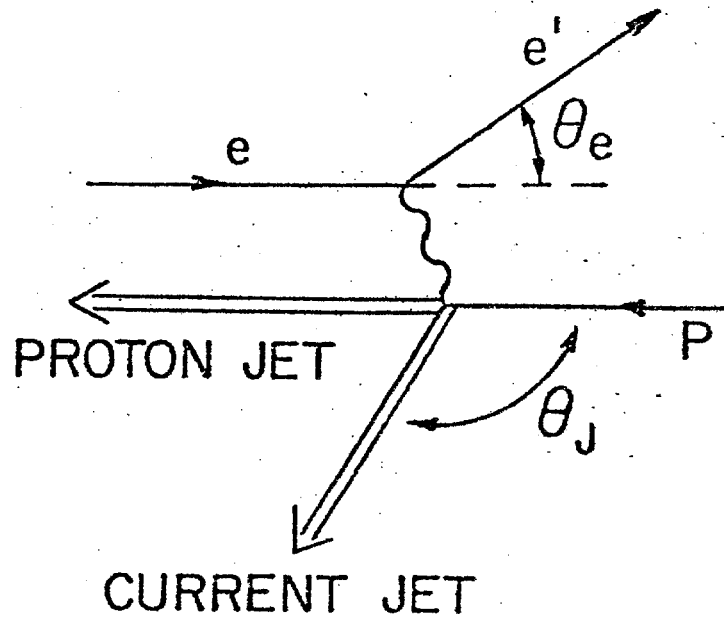
$$Q^2 = -q^2 = -(k-k')^2 = 4E_e E_{e'} \sin^2 \frac{\theta_e}{2}$$

$$m_p v = p \cdot (k-k')$$

$$x = Q^2 / 2m_p v$$

$$y = p \cdot q / m_p v_{\max} = v / v_{\max}$$

We have assumed that the final state consists of a scattered lepton, a current jet which is the materialization of the struck parton, and a target jet which represents the dissociation of the incident proton.



We have the following kinematical relationships for the current jet:

$$P_J = xp + q$$

$$P_{J1}^2 = sx(1-y) .$$

$$\cos\theta_J = E_e y - xE_p(1-y) / E_e y + xE_p(1-y) .$$

B. Comparison with the Tevatron Program

Figures 1a, and 1b, compare the NC and CC event rates expected for the ep facility to those expected in fixed target μ, ν experiments at the Tevatron. The cross sections used in computing the e-p rates are shown in Appendix I. For μ and ν calculations, we assume an incident lab momentum of 600 GeV/c for both the μ and ν and predicate our rates on expected time averaged luminosities (including duty cycle)

of $10^{32} \text{ cm}^{-2} \text{ sec}^{-1}$ for μ 's and $10^{34} \text{ cm}^{-2} \text{ sec}^{-1}$ for ν 's.

Figure 1 shows that the rates expected for the ep facility are considerably larger than fixed target rates for Q^2 exceeding 100 GeV^2 . We thus see that an ep facility opens up kinematical regions inaccessible to fixed target experiments at the Tevatron.

Aside from the obvious advantages of enhanced rate, an ep facility will allow one to study lepton-nucleon scattering with an open geometry. We can thus study the hadronic states accompanying the scattered lepton in considerable detail. For example, we will be able to separate the current jet from the proton dissociation jet, and search for the presence of new quark flavors among the hadrons in the current jet.

The ability to vary the polarization of the incident electron, inherent in an ep facility, offers the additional advantage of allowing us to observe dramatic weak and electromagnetic interference effects.

Next, we elaborate on the physics objectives outlined above.

1) Study of structure of the proton, the quark and the electron.

Using the equations outlined in Appendix I, we calculate the CC and NC rates for the proposed electron target experiment. Figures 2a through 2d show these rates as a function of x and y . In Sec. III, we discuss the separation of charged and neutral current events. We conclude that a

cut on the missing $P_{\perp} > 5 \text{ GeV}/c$ is sufficient to separate the two samples. We also discuss the systematic errors involved in measuring x and y from the current jet.

In addition this facility offers a unique opportunity to study the substructure of the quark. It would not be at all surprising, given the large number of flavors, to find that quarks do indeed have a structure. We can probe distances as small as $5 \times 10^{-17} \text{ cm}$. If the quark has a form factor, we can observe a change in the x, Q^2 distribution of the events. In addition we will measure the neutral current cross section for both charges and helicities. Using the asymmetry parameter least sensitive to the weak interaction effects, we will be able to extract the one photon exchange cross section. If there is a damping of the form $1/(1+Q^2/M^2)^2$ due to quark structure, we will be able to observe it if $M \leq 0.5 \text{ TeV}$ (for six weeks of running).

2) Weak and electromagnetic interference effects.

We will be able to demonstrate the presence of the weak and electromagnetic interference through the measurement of asymmetry parameters. The available polarization allows us to measure the parity violating asymmetry, which is expected to be $\approx 25\%$ at $x = 0.5, y = 0.5$, in a region where we have appreciable rates. The magnitude of this asymmetry can be compared to the fixed target asymmetry, which is $\approx 10^{-4}$. In addition, the availability of both electrons and positrons will enable us to measure additional asymmetries (Fig. 4).

Such measurements allow one to determine the relative strengths of the vector and axial vector terms.

3) Propagator effects.

As a new kinematical region is opened up, where propagator effects become apparent one might expect that these propagator effects might be very complex, e.g. several intermediate bosons. We believe that we will have the ability to disentangle a new complex situation. If the mass and coupling of the lightest W are known, it is possible for this experiment to detect the effects of an additional W up to mass $M_W \leq 350$ GeV. Similarly if the mass and coupling of the lightest Z^0 is known, we will be sensitive (through charge asymmetry) to the effects of additional Z^0 's, up to a mass $M_Z \leq 750$ GeV.

4) Search for right handed charged current.

In the simplest version of the W-S model ($SU(2)_L \times U(1)$), there is only left handed charged current. However nature could very well be left-right symmetric. Since present data at low Q^2 matches the $SU(2)_L \times U(1)$ model to a few percent, the mass of a right handed propagator has to be greater than 200 GeV. Hence as one approaches high Q^2 the ratio of right handed to left handed current events would increase, resulting in increased sensitivity. We should be sensitive to these new currents up to propagator mass of ~ 350 GeV. For example, for $M_{WR} = 350$ GeV the rate with e^-_R for $Q^2 > 1000 \text{ GeV}^2/c^2$ is 94 with a background of 730 events. The 730 events come from e^-_L contamination. (We assume 90% pure e^-_R beam, 6 weeks of running.)

5) Time reversal invariance.

In addition to having circularly polarized beams, it is also possible to work with transversely polarized electrons. By measuring $\vec{\sigma} \cdot (\vec{P}_{in} \times \vec{P}_{out})$, where $\vec{\sigma}$ = polarization of e, \vec{P}_{in} = incoming electron momentum, \vec{P}_{out} = momentum of any one of outgoing particles, it will be possible to detect any T violation, which may arise from the Higgs mechanism, etc.

6) Electroproduction of heavy quarks at high Q^2 .

In the limit of high Q^2 , all quark flavors (u, d, s, b, t ...) are expected to equally populate the quark-antiquark sea. Previous estimates,⁷ based on simple generalized vector dominance model considerations, conclude that the production of particles containing a top quark, should occur at the 10% level in interactions with a Q^2 greater than 500 GeV².

We have computed the expected yield of particles containing heavy quarks using the Altarelli-Parisi equation:

$$\frac{d}{dt} P_n^i(t) = \gamma_n^{ij}(t) P_n^j(t)$$

where $t = 1/2 \ln Q^2/\Lambda^2$, P_n is a vector of the n^{th} moment of the parton distributions ($i, j = g, u, \bar{u}, d, \bar{d}, \dots$) and γ_n is the matrix of anomalous dimensions, which is dependent on the running coupling constant g^2 . Georgi and Politzer⁸ have calculated γ for heavy quarks to first order in QCD theory. Figure 5 shows the parton momentum fraction carried by the quarks where we have taken $m_b = 5$ GeV and $m_t = 15$ GeV.

By fitting the calculated moments to functions similar to those of Buras and Gaemers, we obtained the yields shown below in Table I.

In addition to computing the rates for liberating heavy quarks already present in the sea by the neutral current, we are studying the rates for converting a lighter quark existing in the sea into a heavier quark via the charged current. For example, if the t quark were considerably heavier than the b quark, the rate for converting a b quark into a t quark via W exchange might dominate over the rate for liberating a t quark out of the sea via the neutral current.

In the region of low x and high Q^2 (where new flavor production occurs), the current jet and incident electron are well separated. Hence we will be able to identify the production of heavy quarks through their semileptonic decays into leptons with high P_{\perp} with respect to the current jet axis. The purely hadronic decays are expected to produce a broadening in the jet.

7) Photoproduction.

Electroproduction in the limit of small Q^2 can be described as the radiation of an almost real photon followed by the interaction of the photon with the proton. The intensity of the beam is given by the Weizäcker-Williams formula:

$$kN(k) dk = \frac{\alpha}{2\pi} \left(\frac{E^2 + E'^2}{E^2} \right) \ln \frac{Q_{\max}^2}{Q_{\min}^2} dk ,$$

where E and E' are the energies of the incident and scattered electron, and $Q^2 = EE' \theta_e^2$. The number of l^- vector mesons and bare quarks produced per day is shown below.⁹

	mass (charge) (GeV)	σ_{Tot}	Events/day
$\gamma+p \rightarrow J/\psi^+ \dots$	3.1	30 nb	26,000
$\gamma+p \rightarrow T^+ \dots$	9.4	90 Pb	80
$\gamma+p \rightarrow C^+ \dots$	1.5 (2/3)	1 μb	900,000
$\gamma+p \rightarrow b^+ \dots$	4.5(-1/3)	27 nb	8,000
$\gamma+p \rightarrow t^+ \dots$	15 (2/3)	10 nb	900

These vector mesons will have small laboratory longitudinal momentum, and will therefore be easy to detect. Furthermore, as the Q^2 of the event increases, the cross section contribution from low mass vector mesons such as the ρ is suppressed relative to the contributions from the heavier vector mesons such as the T .

8) Hunt for new and exotic particles.

The list of new, exotic particles predicted in modern theories continues to grow. Because of the flexibility of the ep facility, it will be possible to look for many of these particles. We have unique capabilities for producing and detecting heavy leptons with the electron quantum number, and leptoquarks which are required in current grand unification schemes. Both particles will have dramatic signatures.

Table I

<u>Mass</u>	<u>Charge</u>	<u>Q_o^2</u>	<u>events/month (3×10^6 sec)</u>
5	-1/3	25	2.7×10^5
15	+2/3	225	1.0×10^4
20	+2/3	400	2.3×10^3
30	+2/3	900	2.1×10^2
50	+2/3	2500	3

Note that the above rates are calculated for the region $Q^2 > m_H^2$, where the renormalization group arguments are valid. There will be heavy quark production in the region $Q^2 \leq m_H^2$. As such, the above rates are a lower limit.

III. The Lepton-Quark Experiment

A. Introduction

In this section we intend to show that a general e-p detector, capable of handling a wide range of interesting physics, is feasible. It could be built today, with present well tested experimental techniques. We will show that the rate requirements are modest, the backgrounds are easily overcome, and that the triggering rate is comparable to present fixed target experiments rates. We will show that this detector is capable of doing the deep inelastic physics. Also many of the new phenomena outlined earlier will have spectacular signatures in this detector.

In this section, we discuss the requirements of a detector which can:

(1) Separate neutral ($ep \rightarrow e'X$) and charged ($ep \rightarrow \nu X$) current interactions.

(2) Measure the scaling variables x, y for both reactions. Note that a measurement of x, y is equivalent to an \bar{x} and Q^2 measurement, hence structure functions can be determined.

(3) Detect the low Q^2 reactions ($Q^2 < 10 \text{ GeV}^2/c^2$) which we call photoproduction.

For the purposes of this discussion, we assume a $15 \times 1000 \text{ GeV}^2$ e-p machine, and limit ourselves to 10 meter space in the intersection region. All throughout the discussion we assume a luminosity of $10^{32} \text{ cm}^{-2} \text{ sec}^{-1}$.

The rates quoted here are in events/day (for a luminosity of $10^{32} \text{ cm}^{-2} \text{ sec}^{-1}$). We have a total of about 3×10^6 $ep \rightarrow e'X$ events, and 1000 $ep \rightarrow \nu X$ per day, with $Q^2 > 3 \text{ GeV}^2/c^2$. To study the details of the detector's response to the simulated events, we have fragmented the current and target jets into stable particles ($\pi, K, p, n, e, \mu, \nu, \gamma$). We chose the Field-Feynman technique,¹⁰ Appendix III.

In the discussion to follow, the momenta of the particles are given in the right handed coordinate system where the positive z axis ($\theta = 0$) is the electron direction, while $\theta = 180^\circ$ is the proton direction.

B. Separation of Neutral and Charged Current Events

The selection of charged current events relies on the large P_\perp imbalance characteristic of a missing neutrino. Missing P_\perp , however, can be due to the resolution in detecting the energy and angle of the hadrons in the final state. We have incorporated these effects into a Monte Carlo program, which shows that in neutral current events the P_\perp imbalance is $< 5 \text{ GeV}/c$. A cut on the missing P_\perp of $5 \text{ GeV}/c$ should leave us with no neutral current events and with $\sim 90\%$ of the charged current events. Furthermore electron identification by the shower counters should achieve π/e separation of 10^{-3} . The missing P_\perp and the missing electron are sufficient to obtain a clean sample of charged current events.

C. Scaling Variable Measurements

The scaling variables x and y can be extracted from the energy and angle of the outgoing electron, or alternately from the energy and angle of the current jet. In Figs. 6a-d we show the energy and angle of the outgoing electron and jet as a function of x for several values of y . Note that the target jet is assumed to have zero P_{\perp} .

(1) In the low y region the electron energy is a slowly varying function of x . As such the error in x , at low y , will be dominated by the electron energy resolution, Fig. 6a.

(2) In the high y region, the electron angle is a slowly varying function of x (for $x > 0.1$). The error in x , at high y , will be dominated by the electron angle measurement, Fig. 6b.

(3) In all regions of y , the current jet angle is a slowly varying function of x ($x > 0.2$). The error in x will therefore be dominated by the angular resolution of the jet axis, Fig. 6d.

(4) For very low y ($y < 0.01$) the jet axis is very close to 180° . Hence there will be problems due to the loss of some or all of the jet particles down the beam pipe. Figure 7b shows the lines of constant jet angle in the x - y plane corresponding to 100, 50, 25 mrad with respect to the proton beam. Note that x and y are shown on a log-log scale, with y going up to only 0.1. The x and y regions below these lines are inaccessible for x and y measurement, if the beam pipe subtends 200, 100, 50 mrad, respectively. This means that one has no information about the very low Q^2 region ($Q^2 = 60 - 300 \text{ GeV}^2/c^2$) for charged current events.

(For neutral current events, we can use the lepton variables.) It is however desirable to reach low enough Q^2 to link with fixed target experiments ($Q^2 \sim 100 \text{ GeV}^2/c^2$). This can be done by lowering the proton beam energy. For example in 15 x 500 data, one can reach a factor of ~ 2 smaller Q^2 for the same beam pipe diameter (see Fig. 7a).

We have studied the effect of energy and angular resolution on the systematic errors in x and y measurement. Figures 8a, b shows the x-y (1σ) errors obtained from the electron the current jet variables, using the resolution of the detector outlined in Sec. D. We believe that a detector capable of accurately measuring x and y must have excellent electron energy resolution at small y (or at small angles), and excellent angular resolution throughout the entire detector.

D. The Proposed Detector

Figure 9 shows the schematic of the proposed e-p detector. It consists of three detectors covering the forward (electron) direction ($0 \leq \theta \leq 45^\circ$), the central region ($45^\circ \leq \theta \leq 160^\circ$), and the backward (proton) direction ($160^\circ \leq \theta \leq 180^\circ$). The choice of the angles covered by each detector, as well as the choice of the elements of each detector, is predicated on the kinematical and rate considerations outlined earlier. Figure 10 shows the regions of the x-y scaling variables regions covered by each detector for both the scattered lepton and current jet.

Next we discuss the details of each of the three detector systems. We especially emphasize the rate capability, energy and angular resolution of each detector.

E. The Electron Detector

This detector covers the region $0 \leq \theta \leq 45^\circ$, where the rates will be ≤ 1 KHz (ref. Fig. 12 for the electron angular spectrum). Since this detector covers the low y region (Fig. 10), the energy resolution is of crucial importance. We propose a 3 m x 3 m lead glass array, with a central 1 m x 1 m sodium iodide array. The block size will be 5 cm x 5 cm, for a total of 3600 channels. The angle resolution (1 mrad) will be obtained by a series of 3 mm spacing wire chambers placed in front of the array. This array is capable of energy resolution of $\sigma_E/E = 0.05/\sqrt{E}$. Two reasons motivate placing sodium iodide at the center of the array:

- (1) improving the energy resolution in the low Q^2 region,
- (2) keeping the lead glass well away from the synchrotron radiation background which could over a period of time cause yellowing of the lead glass.

A small fraction of the hadrons reach the electron detector (see Fig. 13 for the hadron angular spectrum). These come from the low x high y region, where the angle of the jet is rapidly varying with x and y . Therefore the detector designed to catch these hadrons need not have excellent angular resolution. We propose a 2 in.-1/2 in. segmented iron-acrylic scintillator calorimeter, with

about 150 mrad angular segmentation. The energy resolution of this detector will be of order $\sigma_E/E = 0.50-0.75/\sqrt{E}$. Note that there is no region in the x-y space where both the scattered electron and the current jet lie in the electron detector. This is a welcome simplification.

F. The Central Detector

The energy spectrum of the hadrons from the current jet fragmentation (Fig. 14) is such that it is best matched by a magnetic detector. We have considered two magnet configurations: solenoidal and dipole. We find that a solenoidal geometry has the best and most uniform acceptance in the region of moderate Q^2 (a few thousand GeV^2/c^2), and in addition has minimum interference with the beams. A coil configuration similar to the proposed Fermilab \bar{p} -p detector (5m long, 3m diam.) is suggested. A superconducting coil of this size is capable of delivering magnetic fields of up to 1.5 Tesla. With the intersection region displaced 1 m toward the electron detector, this configuration covers the angles $45^\circ \leq \theta \leq 160^\circ$. With this displacement of the intersection region, the bulk of the forward electron counting rate falls in the specialized electron detector. Also the solenoid's acceptance for the current jet is made larger.

Inside the coil lies a tracking system. The outside of the coil is surrounded by electromagnetic and hadron calorimeters.

1. The Tracking System

We propose a cylindrical drift chamber for the tracking system. A drift chamber with 1 cm drift cell and 10,000 channels will be capable of 300 μm resolution, or $\sigma/P_{\perp} \sim 0.001 P_{\perp}$. We expect to do most of our running with $B = 0.5$ Tesla.

In addition one can place a small proportional chamber, with wires perpendicular to the beam direction, around the interaction region. This chamber will locate the interaction vertex and help eliminate beam-gas events.

G. The Electromagnetic Calorimeter

As we emphasized earlier, the current jet angular resolution is crucially important, especially in charged current events where the jet variables are used to extract the scaling variables. The current jet multiplicity is equally divided between charged tracks (whose angles are measured with great precision in the drift chamber), and gamma rays (whose angles are measured in the shower counter). Consequently the angular resolution of the jet will be dominated by the angular resolution of the shower counter. The necessity of a calorimeter with fine segmentation makes a proportional counter an especially attractive choice. Recently we tested a (1/4 in.) lead gaseous argon induced charge readout calorimeter.¹¹ We obtained energy resolution

of $\sigma/E = 0.2/\sqrt{E}$ and an angular resolution of the shower center of better than $1/3$ of the cell size. We believe that the resolution can be improved to $\sigma/E = 0.15/\sqrt{E}$. This is fairly close to the $\sigma/E = 0.1/\sqrt{E}$ obtained by lead scintillator. However, the economy, ease of construction and calibration, and the fine segmentation makes the lead-argon calorimeter very attractive. We propose to build sixteen 250 cm x 120 cm modules to be arranged in octets (see Fig. 15). Each module covers 1 radian in θ , and $\pi/4$ radian in ϕ . With 2 cm x 4 cm segmentation, one can obtain 8 mrad θ segmentation and 25 mrad ϕ segmentation. The readout is done after 1, 6, 20 radiation lengths to achieve $\sim 10^{-3} \pi/e$ separation. The total θ channels/module = 128×3 , ϕ channels 32×3 , or $\theta + \phi = 480$ /module. The counter would have 7,680 ADC channels.

H. The Hadron Calorimeter

The hadron calorimeter will measure the neutral hadrons as well as the very high energy charged tracks measured poorly by the magnetic detector. In the spirit of the electromagnetic detector, we propose an (1 in.) iron-argon calorimeter; sixteen modules each 250 cm x 180 cm. The θ segmentation is 15 mrad, while the ϕ segmentation is 50 mrad. The total number of ADC is 1280. Recently a Stanford-Wisconsin¹² group tested a similar counter, and obtained $\sigma/E = 0.75/\sqrt{E}$.

I. The Backward (Proton) Detector

This detector, which covers the region $160^\circ \leq \theta \leq 180^\circ$, will rely entirely on calorimetry. It is difficult to match a magnetic detector in this region with the machine requirements. We envision a 3 m x 3 m gas calorimeter, with a design similar to the central calorimeter. Longitudinally, the detector will consist of a 20 rad length (1/4 in. lead) electromagnetic calorimeter, followed by 4.5 absorption length (1 in. iron) hadron calorimeter. The segmentation in both x and y will be 1 cm (~ 3 mrad). In each detector the energy is sampled longitudinally five times. The total number of ADC is 6000.

This detector will scan the high Q^2 region for both leptons and hadrons (rate ~ 1 Hz), the low Q^2 region for hadrons (rate ~ 1 KHz), and upstream beam gas interactions (rate is 1 KHz for 10^{13} protons and 10^{-10} Torr).

J. Performance of the Detector

With the resolution outlined earlier, we examined the x-y scaling variables systematic errors. Figure 10 shows the errors due to x-y extraction from lepton and jet variables. It is clear that x-y extraction with low systematic errors is possible, even in charged current events. The very large x-y region has the worst systematic errors when jet variables are used. However in this region it is the statistical errors not the systematic errors that will dominate. For example, at $x = 0.8$, $y = 0.8$, the rate for 100 day run is only ~ 10 charged current events.

K. Background Sources

We intend to make an extensive examination of the background sources as soon as the machine parameters are precisely defined. For now, we rely on the examination of the background sources in HERA. The authors conclude that with suitable placing of simple veto counters, background rate from beam gas interactions can be reduced to ~ 100 Hz. At this low rate, selective triggering is then possible.

L. Instrumented Machine Elements

It is necessary to have a calorimeter placed behind the proton detector in order to capture some of the target jet energy, and possibly measure its P_{\perp} . This will likely be a one or more machine element whose iron laminations are interspersed with scintillator. We are at present studying the requirements of this detector. We will come up with a detailed design as soon as a complete layout of the machine element is finished. We consider the correct design of this detector of utmost importance to the success of the experiment.

M. Conclusion and Costs

An e-p detector capable of measuring both neutral and charged interactions is feasible. The detector is relatively simple to construct, requiring no new advances in detector technologies. The reliance on gas calorimetry serves the dual purpose of providing the necessary angular segmentation and simplifying the construction of the detector. The cost of gas calorimetry is also lower than scintillator or liquid argon.

We provide a list of the essential detectors as well as an estimate of their cost. We believe that the cost is ~ 7 million 1980 dollars.

IV. The Electron Target and Interaction Area

Fermilab has tentatively decided that the ep interaction area should be located at straight section D, and has expressed a strong preference that the electron ring should not be in the Main Ring tunnel but rather should be in a separate tunnel tangent to the Main Ring, see Fig. 16. Designing a 10-15 GeV electron or positron storage ring is relatively straightforward because by now numerous very similar rings such as CESR or PETRA have been built and are in operation. What is difficult is to bring the electrons into collision with the 1 TeV protons of the Tevatron in the rather short straight section (~ 50 m) that is available. Polarization of the electron beam is an eventual requirement which adds a degree of complexity to the problem. We are also seeking an economical design which does not compromise either performance or reliability.

Happily, Tom Collins of Fermilab has made a design of the electron ring in which he has solved the problem of bringing the electron beam into collision with the Tevatron beam for an electron energy of 10 GeV (see addendum by Collins). He has also expressed confidence that after such a ring has been in operation, it should be possible to increase the electron energy on the basis of the experience acquired.

Collins calculates a basic luminosity of $1.5 \times 10^{31} \text{ cm}^{-2} \text{ sec}^{-1}$, but he suggests a number of improvements such as a low β insertion, rebunching the beam into fewer buckets, and using a larger electron current (at the cost of more rf power).

All of these he estimates would raise the luminosity to about $2 \times 10^{32} \text{ cm}^{-2} \text{ sec}^{-1}$. It thus appears that the canonical value of luminosity, $10^{32} \text{ cm}^{-2} \text{ sec}^{-1}$, is a reasonable one to use in computing counting rates, but the present experience with storage rings would indicate that a few times $10^{31} \text{ cm}^{-2} \text{ sec}^{-1}$ might be more realistic.

As shown in Fig. 16 the electron ring is of racetrack design in which the curved parts of the tunnel have an average radius of 150 m and the length of each of the two straights is 100 m. The straight α is long enough to bring the electron beam into collision with the proton and to transpose the normally transversely polarized beam into a right handed or left handed polarized beam while in the interaction region and then transpose it back to its original direction. There are a number of ways of accomplishing this: we favor using a very strong longitudinal field in which the direction of polarization precesses by 90 degrees; then a short length of horizontal bending magnet would cause the beam to precess to a direction parallel to the beam. The mirror image of this would restore the polarization. We favor this method because the polarization can be changed by simply reversing the magnets. We do not claim to be able to use polarization in the first experiment because we have not yet calculated the necessary accuracy of the magnets nor, alternatively, have we invented an appropriate feedback mechanism for controlling the magnets. Given the importance

and uniqueness of polarization experiments, it is imperative that we eventually achieve this mode of experimentation. We will allow adequate space for whatever beam gymnastics are required.

In the same vein, we expect eventually to have a positron beam instead of the electron beam, but we will not have it in the first experiments. If necessary, we could duplicate the Cornell arrangement used in CESR for ratcheting buckets of positrons into one or a few bunches. It would be more desirable to have a small booster accelerator to bring the electrons or positrons to a few GeV at which energy the size of the beam would rapidly dampen. By rapidly cycling the booster, a number of successive pulses could then be injected from a 50 MeV injector linac. This booster and its linac would be placed at the outer straight section. The positron part of the booster would be added at a later time.

The rf acceleration will essentially be a copy of that used at Cornell except to be scaled up from 8 to 10 GeV and scaled down for the 50% larger radius. This implies a beam energy loss per turn of about 10 MeV/turn instead of Cornell's 6.56 MeV/turn. The design current in both machines is also the same, 0.2 mA, hence the number of cavities at Fermilab will have to be increased from CESR's 4 to 6, giving a total length of about 25 m which would fit easily into the 100 m long straight section. To reach 15 GeV implies about 40 MeV/turn which would obtain by quadrupling the length of the

cavities to 100 m, but that would leave no space for other necessary devices such as quadrupoles and injection magnets. Perhaps there would be enough space for 80 m of cavities plus the use of more rf power to get the necessary voltage. That implies going from a power usage of about 3.6 MW at 10 GeV to about 18 MW at 15 GeV. To run at or above 15 GeV in this ring would most likely require superconducting rf cavities.

The tunnel, cut and fill, would be built of horseshoe shaped precast concrete sections, 8 ft wide by 8 ft high. Building it of circular sewer sections with a flat floor poured in place might be cheaper. The plane of the ring would be tilted in such a way that it would touch the Main Ring at the proton side but that the other straight section with rf equipment and injector would be closer to the surface (electrons do not produce much radiation). This might reduce the cost of the tunnel, and would certainly produce better drainage. A building 100 m long and about 20 m wide (about 10^4 square feet) would be constructed just inside the outer straight section. One million dollars has been allowed for this building assuming a minimal cost of \$50 per square foot. It would be possible to reduce the size of this building by a factor of two if necessary.

It is assumed the experimental area at straight section D of the Main Ring has already been funded. Nevertheless,

funds are being requested to allow for the electron ring to be joined to the experimental area.

The lattice of the magnet ring is shown in Figs. 4 and 5 of the addendum by T. Collins. In calculating the cost of the magnets, it has been assumed that the construction would be identical to that of CESR except to be 1.5 times greater in length. In fact because of eddy currents in the aluminum donut, it might take too long to accelerate the electrons from the few GeV of the booster to 10 GeV. The substitution of a stainless steel donut lightly gold plated on the inner surface would probably not be more costly and would allow the acceleration in a reasonable time.

V. Cost Estimates and Schedule

The design of the electron ring will closely follow that of the CESR storage ring at Cornell University. Thus most of the costs can be scaled and inflated rather straightforwardly. The tunnel and building costs are taken from the most recent experience at Fermilab. The cost estimates are shown in Table I: the first column showing the Cornell costs for 1977 (reestimated for actual experience for the rf cavities), the second column shows the estimates for 10 GeV electrons inflated to 1980 values, and the third column shows the estimates for 15 GeV also in 1980 dollars. Of course the estimates are very rough and do not allow for improvements which ought to reduce the costs.

The cost of the detector is shown in Table II. It is based on etc. etc.

Roughly, this can be summarized to indicate that the ring will cost about \$20M and the detector about \$7 M. Then if \$2 M are left for contingency, we get the \$10 M per year for three years indicated in the introduction. An additional year with \$10 M should allow us to operate and bring the energy up to 15 GeV. Because the rf cost is dominant and because it is constructed in a linear fashion, it can absorb some share of the contingency, implying the possibility of operating at a slightly lower energy in view of the E^4 dependence of the radiation loss.

The schedule calls for bringing the experiment into operation in 1984. This implies the \$10 M per year figure assuming funding were to start in 1981. If it were to start in 1982, then \$15 M per year for two years would become desirable. Much beyond that will involve severe geriatric problems to at least one of the experimenters.

Item	8 GeV	10 GeV	15 GeV
	$\bar{R}=100$ m	$\bar{R}=150$	
	Cornell 1977 \$ (in K)	1980 \$ (in K)	
Magnets	1150	2360	1750
Power Supplies	225	340	560
Vacuum	945	2440	1800
Injector		3000	3000
rf	1747 +112	3800	9000
Controls	930	1350	1000
Tunnel		2750	2750
Bldg		1000	1000
Utilities (5 MW)			

Costs

Assumed Prices

1 in. steel, 2 in. steel	\$2,000, \$1,500/ton
1/4 in. lead	1,500/ton
ADC	\$40/channel
TDC + Cables	\$30/channel
Lead Glass	\$100/1000 cm ³
PM 2 in. tube	\$100
PM 5 in. tube	\$200
MWPC readout	\$20/channel
NaI	\$1000/1000 cm ³

List of DetectorsMagnet

Length	5 m
Diameter	3 m
Maximum field	1.5 Tesla

Electron DetectorLead Glass Array

Size	3 m x 3 m x 60 cm
Segmentation	5 cm x 5 cm
# of Channels	3600

Hadron Calorimeter

Size	3 m x 3 m x 1 m
# of 2-in. steel plates	15
# of 1/2 in. acrylic scintill.	15
Segmentation	30 cm x 30 cm
# of Channels	100

Wire Chambers

# of Planes	4
Spacing	3 mm
# of Channels	4000

Central DetectorDrift Chamber

Drift Cell Size	1 cm
# of Cells	10,000

Shower Counter

Sixteen 8 ft x 4 ft modules		
ϕ Segmentation/module	25 mrad/channel	32 channels
θ " "	8 " "	128 "
z " "	3 (1,6,20 r.l.)	
# of Lead Plates (1/4 in.)		20
Total # ADC's		7,680

Hadron Calorimeter

Sixteen 8 ft x 6 ft modules

ϕ Segmentation/module	50 mrad/channel	16 channels
θ " " "	15 " "	64 "
# of Steel Plates (1 in.)		30
Total # ADC's		1,280

Forward DetectorElectromagnetic Detector

x Segmentation	300
y Segmentation	300
z Segmentation	5
Total No. of ADC's	3,000
Number of Lead Plates (1/4 in.)	20

Hadron Calorimeter

x Segmentation	300
y Segmentation	300
z Segmentation	5
Total No. of ADC's	3,000
Number of Steel Plates (1 in.)	30

	<u>Cost</u>
<u>Magnet & Yoke</u>	1 M
<u>Electron Detector</u>	
Lead Glass/NaI	500 K
PM (2 in.)	350 K
ADC	150 K
Steel (50 tons)	80 K
PM (5 in.)	20 K
ADC	4 K
Chamber Electronics	120 K
<u>Central Detector</u>	
TDC	300 K
ADC Shower Counter	300 K
ADC H.C.	50 K
Pb (70 tons)	100 K
Iron (500 tons)	1000 K
<u>Forward Detector</u>	
ADC	250 K
Lead (10 tons)	15 K
Steel (50 tons)	100 K
Mechanical Support & Construction Costs	~ 2 M
Computer & Trigger	800 K
<u>TOTAL</u>	<u>7.1 M</u>

VI. Study of Running Eight Weeks in 1984

A six week run with $10 \times 1000 \text{ GeV}^2$ (unpolarized electrons) would result in $\sim 5 \times 10^7$ $ep \rightarrow e' \dots$ and 15,000 $ep \rightarrow \nu \dots$ events with $Q^2 > 3 \text{ GeV}^2/c^2$. A two week run at $10 \times 500 \text{ GeV}^2$ would follow. The combined data sample will permit a detailed bias-free determination of the structure functions. We will be able to find if QCD is indeed a viable theory at large Q^2 . Also R will be measured with a few percent accuracy.

If nothing is known about Z or W masses at that time, then we will be able to determine the mass of the lowest Z and/or W to $\sim 4\%$, if the mass is $\leq 350 \text{ GeV}$. If the mass and coupling of the lightest Z or W are known, then we are sensitive to deviations in the Q^2 distribution due to extra Z or W, up to masses $\sim 350 \text{ GeV}$.

If the quark has radius of order $5 \times 10^{-17} \text{ cm}$ or larger, then the Q^2 distribution, or the structure functions will exhibit a statistically significant deviation from the expected distributions. Pinning down the exact origin of these anomalies will require the availability of positron beams to eliminate possible weak interaction effects.

On a less spectacular but nonetheless important front, we would search for the top quark. Rates should be \sim few hundred if $m_t \sim 30 \text{ GeV}$. No e^+e^- machine will have reached that limit by 1984. We will also accumulate 2×10^8 photoproduction events, which in the past have proven to be a rich source of new particles.

The installation of polarization hardware will not come until the second year. A search for the right hand charge current and study of interference term between electromagnetic and weak interaction will be carried out. Positron will come a year later. Having both charged and helicities will make possible a complete examination of the details of the weak interaction.

We would like to thank Prof. T. D. Lee, Prof. A. Mueller,
Dr. T. Collins and Dr. J. Peoples for many valuable
discussions.

APPENDIX I

Calculation of Rates

We consider the first reaction

$$ep \rightarrow e + x \quad \dots \quad (2.1)$$

The 1γ exchange cross section is

$$\frac{d^2\sigma^{1\gamma}}{dx dy} = \frac{4\pi\alpha^2}{s x^2 y^2} \{ (1-y)F_2(x, Q^2) + y^2 x F_1(x, Q^2) \} \quad (2.2)$$

If we assume Callan-Gross relationship

$$F_2(x, Q^2) = 2x F_1(x, Q^2), \text{ then}$$

$$\frac{d^2\sigma^{1\gamma}}{dx dy} = \frac{4\pi\alpha^2}{s x^2 y^2} (1-y + \frac{y^2}{2}) F_2(x, Q^2) \quad \dots \quad (2.3)$$

In evaluation of $F_2(x, Q^2)$, we used the Buras-Gaemers QCD parametrization of the quarks (see Appendix II).

The reaction (2.1) can proceed via weak and 1γ exchange currents. The differential cross sections which now depend on the helicity and charge of the incoming electron are

$$\frac{d\sigma}{dx dy} = \frac{d\sigma^{1\gamma}}{dx dy} \cdot f(\eta) \quad \dots \quad (2.4)$$

Here $\eta =$
$$\begin{pmatrix} e_L^- \\ e_R^- \\ e_L^+ \\ e_R^+ \end{pmatrix} \quad (2.5)$$

The function $f(\eta)$ is given

$$f(\eta) = \sum_{ij} \xi_{ij}^G \xi_{ij}^p [A_{ij}(x) + \xi_{ij}^B B^{ij}(x) \frac{(y-y^2/2)}{1-y+y^2/2}]$$

$i = 1 \quad j = 1$ corresponds to 1γ exchange term,
 $i = 1 \quad j = 2$
 $i = 2 \quad j = 1$ } corresponds to γ -Z interference, and
 $i = 2 \quad j = 2$ corresponds to Z exchange term .

$$G_{\eta}^1 = \begin{pmatrix} -1 \\ -1 \\ -1 \\ -1 \end{pmatrix} \quad G_{\eta}^2 = \sqrt{2} \begin{pmatrix} -1+2\sin^2\theta_w \\ 2\sin^2\theta_w \\ 2\sin^2\theta_w \\ -1+2\sin^2\theta_w \end{pmatrix}$$

Here G_{η}^i is the lepton coupling to γ or z ,

θ_w is Weinberg angle.

p^i are the propagators and are

$$p^1 = 1$$

$$p^2 = \frac{G_F}{\sqrt{2} e^2} \frac{Q^2 m_Z^2}{(m_Z^2 + Q^2)}$$

$$\xi_{\eta} = \begin{pmatrix} +1 \\ -1 \\ +1 \\ -1 \end{pmatrix}$$

$$A^{ij} = \frac{1}{2} \frac{\sum_k (c_k^{iL} c_k^{jL} + c_k^{iR} c_k^{jR}) (q_k(x, Q^2) + \bar{q}_k(x, Q^2))}{\sum_k e_k^2 [q_k(x, Q^2) + \bar{q}_k(x, Q^2)]}$$

$$B^{ij} = \frac{1}{2} \frac{\sum_k (c_k^{iL} c_k^{jL} - c_k^{iR} c_k^{jR}) (q_k(x, Q^2) - \bar{q}_k(x, Q^2))}{\sum_k e_k^2 [q_k(x, Q^2) + \bar{q}_k(x, Q^2)]}$$

\sum_k is the sum over all quark flavors .

k

c_k^{iL} , c_k^{iR} are the couplings of the γ ($i=1$) and Z ($i=2$) to the left and right handed k -flavor quark .

$$c_k^{1L} = c_k^{1R} = e_k$$

$$c_k^{2L} = \frac{\sqrt{2} e_k}{|e_k|} (1 - 2e_k \sin^2 \theta_w)$$

$$c_k^{2R} = -2\sqrt{2} e_k \sin^2 \theta_w .$$

Next we consider charge current reactions

$$ep \rightarrow \nu + x \quad \dots$$

The differential cross section is

$$\frac{d^2 \sigma_{e^+}}{dx dy} = \frac{G_F^2}{2\pi} S \left[\frac{m_w^2}{m_w^2 + Q^2} \right]^2 \left[(1-y) F_2(x, Q^2) + y^2 x F_1(x, Q^2) \right. \\ \left. \pm y \left(1 - \frac{y}{2}\right) x F_3(x, Q^2) \right] .$$

Note that the structure functions are different for e^- and e^+ . Again, the Callan-Gross relation is assumed

$$\frac{d^2 \sigma_{e^+}}{dx dy} = \frac{G_F^2}{2\pi} S \cdot \left(\frac{m_w^2}{m_w^2 + Q^2} \right)^2 \left[\left(1 - y + \frac{y^2}{2}\right) F_2(x, Q^2) \right. \\ \left. \pm y \left(1 - \frac{y}{2}\right) x F_3(x, Q^2) \right] .$$

Appendix I I

Quark Distribution Functions

The explicit expressions for Q_k , \bar{Q}_k are in accordance with the Buras-Gaemers parametrization, and CHDS neutrino measurements.

$$Q_u = u_v + s$$

$$Q_d = d_v + s$$

$$Q_s = s$$

$$Q_c = c$$

where

$$u_v(x, Q^2) = \frac{3x^{\eta_1}(1-x)^{\eta_2}}{B(\eta_1, 1+\eta_2)} - d_v$$

$$d_v(x, Q^2) = \frac{x^{\eta_3}(1-x)^{\eta_4}}{B(\eta_3, 1+\eta_4)}$$

$$s(x, Q^2) = \frac{P_s}{6} \left(\frac{P_s}{S_3} - 1 \right) (1-x)^{\frac{P_s}{S_3} - 2}$$

$$c(x, Q^2) = \frac{P_c}{2} \left(\frac{P_c}{c_3} - 1 \right) (1-x)^{\frac{P_c}{c_3} - 2}$$

where

$$\begin{pmatrix} \eta_1 \\ \eta_2 \\ \eta_3 \\ \eta_4 \end{pmatrix} = \begin{pmatrix} 0.72 & -1.19 & G\bar{s} \\ 2.8 & 5.06 & G\bar{s} \\ 0.97 & 1.69 & G\bar{s} \\ 3.55 & 5.06 & G\bar{s} \end{pmatrix}$$

with

$$G = 4/33 - 2N_f, \quad N_f = \text{number of flavors,}$$

$$\bar{s} = \ln \frac{\ln Q^2 / \Lambda^2}{\ln Q_0^2 / \Lambda^2}, \quad Q_0^2 = 2., \quad \Lambda^2 = 0.2 .$$

$$P_s = 3/4 D_{22} + 1/4 D_{12}$$

$$P_c = 1/4 D_{22} - 1/4 D_{12}$$

$$S_3 = 3/4 D_{23} + 1/4 D_{13}$$

$$C_3 = 1/4 D_{23} - 1/4 D_{13}$$

$$D_{12} = 0.11 e^{-0.427 \bar{s}}$$

$$D_{13} = 0.009167 e^{-0.667 \bar{s}}$$

$$D_{22} = 0.169 e^{-0.747 \bar{s}} + 0.488 e^{-0.427 \bar{s}} + 0.429$$

$$D_{23} = 0.0028 e^{-1.386 \bar{s}} + 0.1634 e^{-0.609 \bar{s}} - 0.157 e^{-0.667 \bar{s}}$$

$$\bar{s} = \ln \frac{\ln Q^2 / \Lambda^2}{\ln Q_0^2 / \Lambda^2}$$

Appendix III

Fragmentation of Quark Jet

The dressing of the quark jet is done according to the Feynman-Field recipe.¹⁰ The original quark of flavor q and momentum W_0 creates a color-field in which a quark-antiquark pair is produced. The original quark then combines with the antiquark to form a meson, and the process is repeated with the remaining quark. The following rules are observed:

1. The fraction of energy η that the primary quark leaves to the remaining jet is given by

$$f(\eta) = 1 - a + 3a\eta^2 \quad a = 0.88.$$

2. The quark-antiquark pair carry zero net P_{\perp} , but each has P_{\perp} that is gaussian with σ of 350 MeV/c. The flavor of the $q\bar{q}$ pair is 40% u, 40% d, and 20% s.

3. The process is stopped when the momentum of the remaining jet around the original jet direction is ≤ 0 .

4. The resulting mesons are 50% pseudoscalar, 50% vector.

References

- 1 A. Ruggiero, Report on ep Colliding Beam Facility, Batavia (April 1978).
- 2 BNL Proposal 50648, Brookhaven (April 1977).
- 3 CHEEP Report, CERN 78-02.
- 4 Study of an ep Facility, DESY 79/48 (August 1979).
- 5 S. Kamada et al, IEEE Trans. on Nucl. Sci. NS 74, #3, p. 1194 (June 1977).
- 6 C.Y. Prescott et al, Phys. Lett. 77B, 347 (1978).
- 7 C.H. Llewellyn Smith, B.H. Wiik, DESY Report 77/38 (1977).
- 8 H. Georgi, H. Politzer, Phys. Rev. D14, 1829 (1976).
- 9 H. Fritzsch, K. Streng, Phys. Lett. 72B, 385 (1978).
- 10 R. Field, R. Feynman, Nucl. Phys. B136, 1 (1978).
- 11 E. Hartouni, B. Knapp, Nevis Internal Memo.
- 12 R.L. Anderson et al, IEEE Transactions on Nuclear Sci. NS-25, February (1978).

FIGURE CAPTIONS

- Fig. 1a Number of neutral current events greater than a given Q^2 for 15×1000 and $20 \times 400 \text{ GeV}^2$ facilities compared with a fixed target muon experiment at 600 GeV. Cross sections are calculated for left-handed electrons, with both 1γ and Z exchange.
- Fig. 1b Same as 1a for charged current events. The suppression of the cross section due to the presence of the propagator is also shown.
- Fig. 2a The rate of charged current events in events/day for bins of $\Delta x \Delta y = 0.04$ with Q^2 up to 6×10^4 .
- Fig. 2b Expanded view of the low x region of Fig. 2a showing the event rate for bins of $\Delta x \Delta y = 0.004$.
- Fig. 2c Same as 2a for 1γ exchange.
- Fig. 2d Same as 2b for 1γ exchange.
- Fig. 3 The contributions of the various Z exchange processes relative to the 1γ exchange cross section.
- a) The ratio of γ -Z interference term to the 1γ exchange for incident left-handed electrons.
 - b) The ratio of the $|Z|^2$ term to the 1γ exchange for incident left-handed electrons.
 - c) Same as a) for incident right-handed electrons.
 - d) Same as b) for incident right-handed electrons.

- Fig. 4a The asymmetry parameter $(\sigma(e^-_L) - \sigma(e^-_R)) / (\sigma(e^-_L) + \sigma(e^-_R))$ as a function of y for $x = 0.1, 0.5, 0.9$.
- Fig. 4b Same as 4a for $(\sigma(e^-_L) - \sigma(e^+_L)) / (\sigma(e^-_L) + \sigma(e^+_L))$.
- Fig. 4c Same as 4a for $(\sigma(e^-_L) - \sigma(e^+_R)) / (\sigma(e^-_L) + \sigma(e^+_R))$.
- Fig. 5 Evolution of the second moment ($n=2$) of the parton distributions as a function of $t = 1/2 \ln Q^2 / \Lambda^2$ ($\Lambda^2 = 0.2 \text{ GeV}^2$). The calculation is done according to the prescription of Georgi and Politzer. The $n=2$ moment corresponds to the average fraction of the momentum of the incident proton carried by the partons.
- Fig. 6a-d The energy and angle of the electron and current jet as a function of x for $y = 0.01, 0.2, 0.6, 0.9$.
- Fig. 7a Lines of constant current jet angle with respect to the proton beam. Note the log-log scale ($15 \times 500 \text{ GeV}^2$).
- Fig. 7b Same as a for $15 \times 1000 \text{ GeV}^2$.
- Fig. 8a Scaling variables $x-y$ (1σ) errors obtained from lepton variables using the resolution of the proposed detector.
- Fig. 8b Same as 8a for jet variables.
- Fig. 9 A schematic of the detector.
- Fig. 10a The shaded regions indicate the $x-y$ regions where the current jet will be in the electron, central, and proton detectors.
- Fig. 10b Same as a) for the lepton.
- Fig. 10c The overlap of a) and b).

- Fig. 11 A sample of Monte Carlo events in 5m x 3m solenoidal field with $B_z = 15$ kG. The fragmentation of the current and target jets is done according to Feynman and Field. The electron beam direction is to the right; the proton beam direction is to the left.
- Fig. 12 The electron angle spectrum.
- Fig. 13 The track angle spectrum. Field-Feynman fragmentation is used. The shaded region is the target jet contribution.
- Fig. 14 The track energy spectrum. Field-Feynman fragmentation is used.
- Fig. 15 Sixteen shower counter modules arrangement.
- Fig. 16 The electron ring at Fermilab.

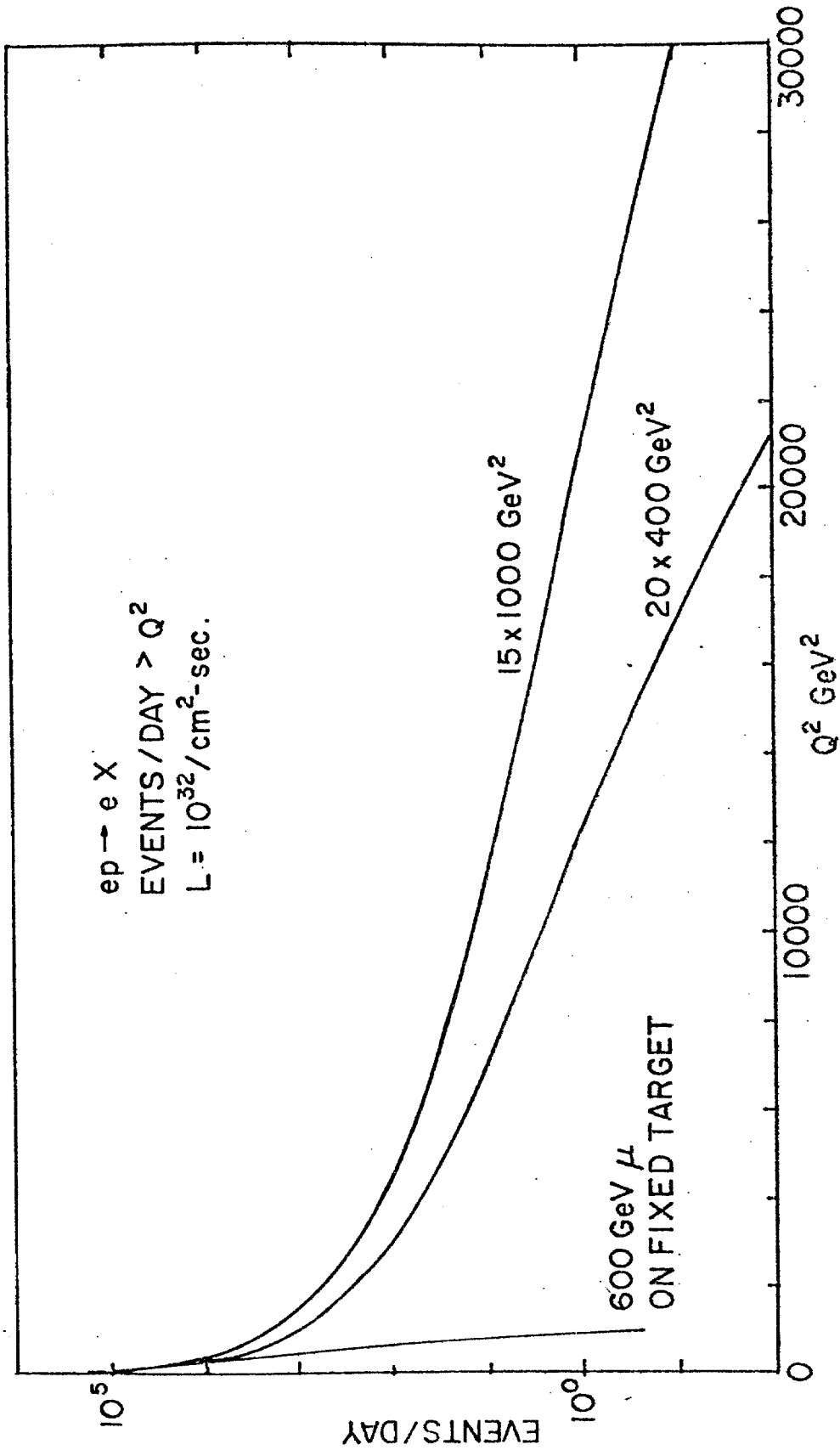


FIG. 1a

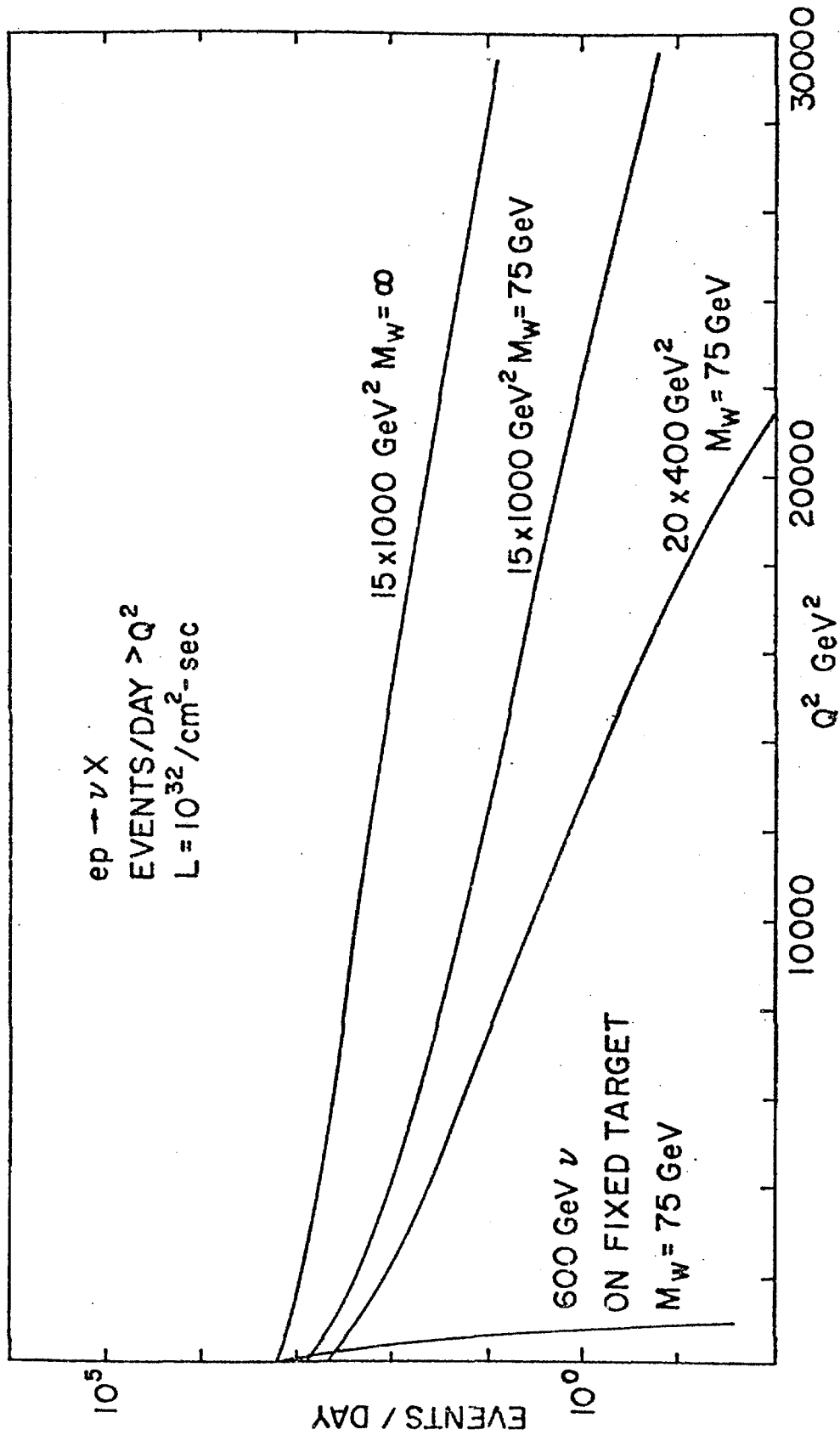


FIG. 1b

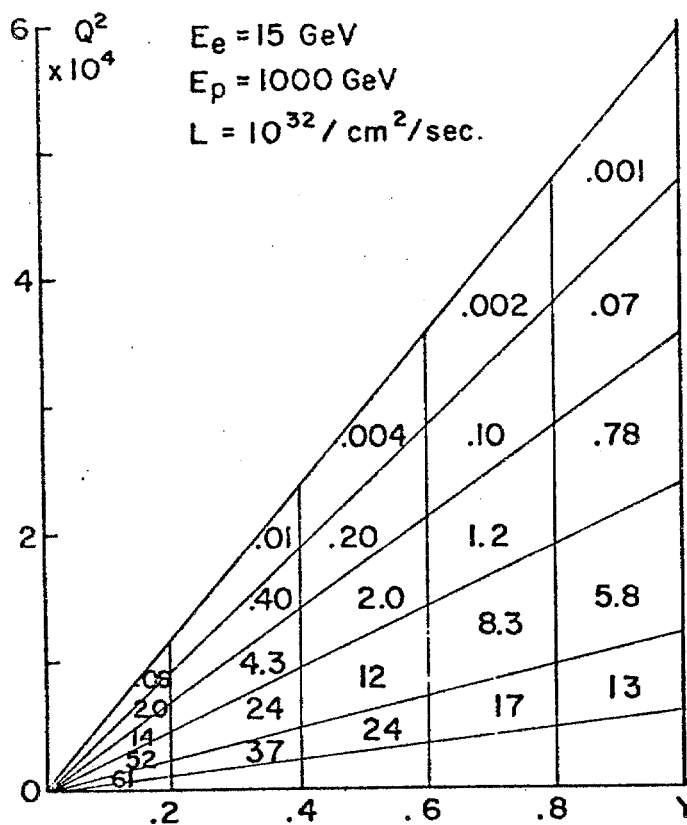


FIG. 2a

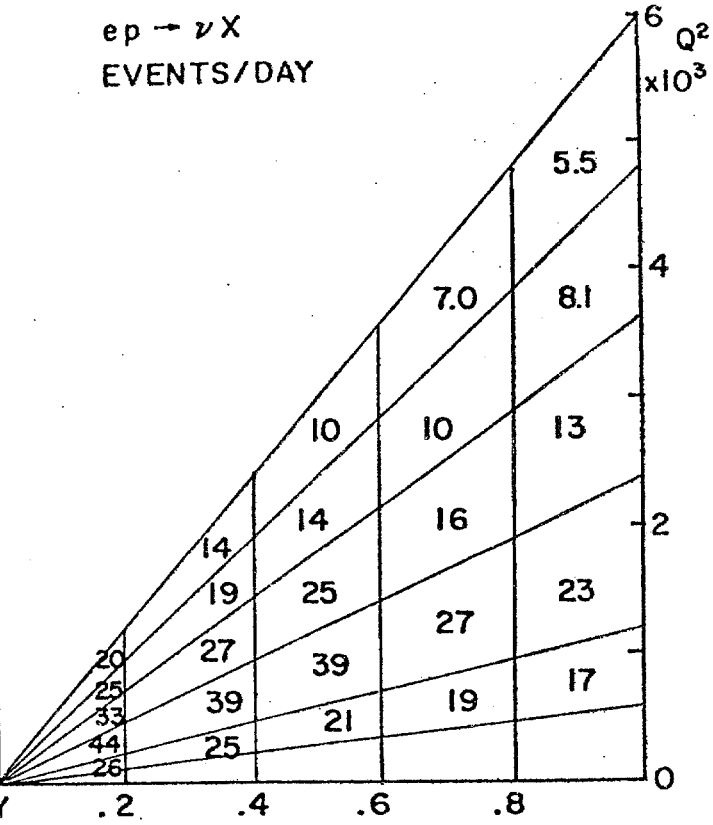


FIG. 2b

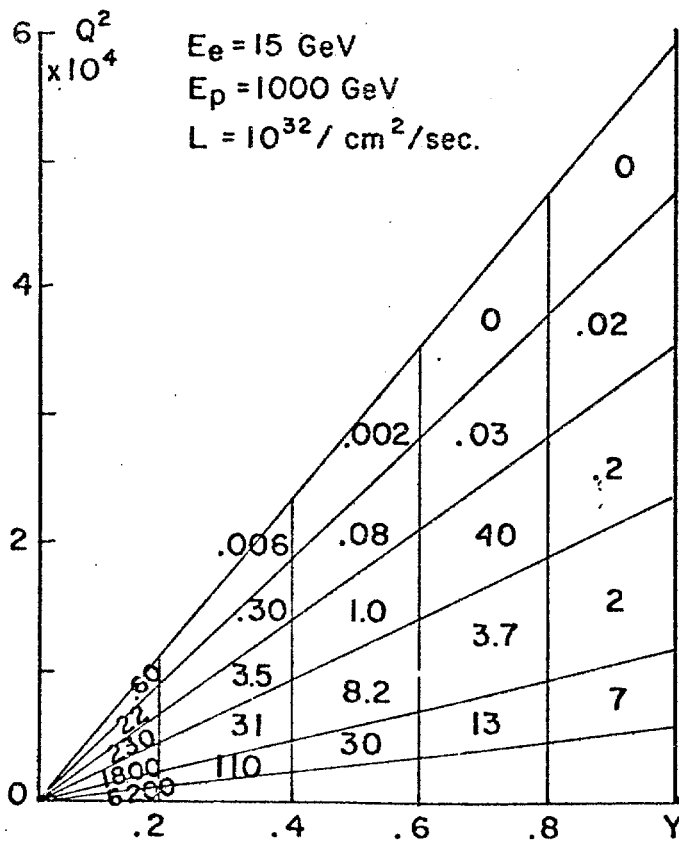


FIG. 2c

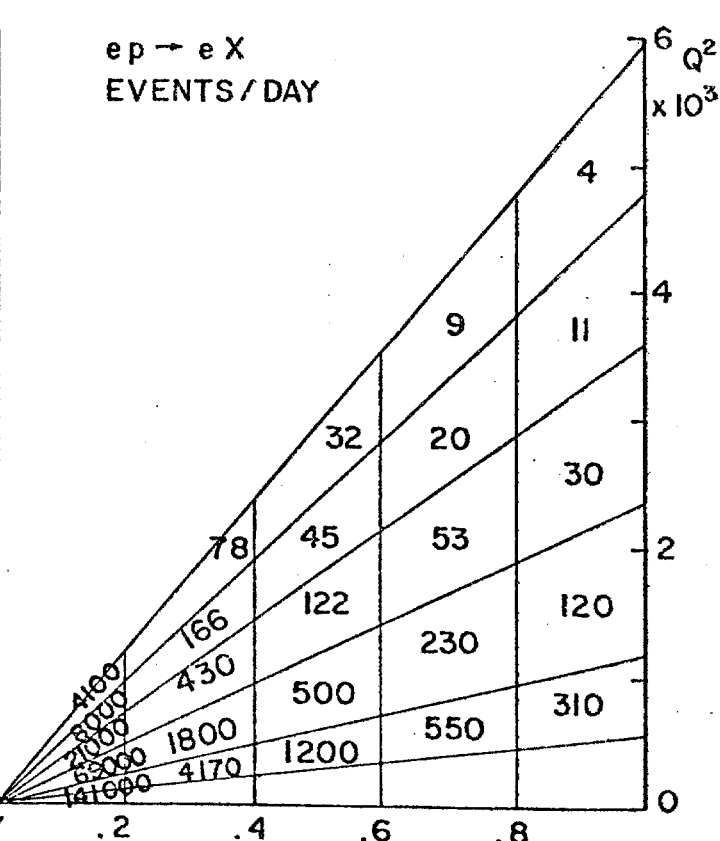


FIG. 2d

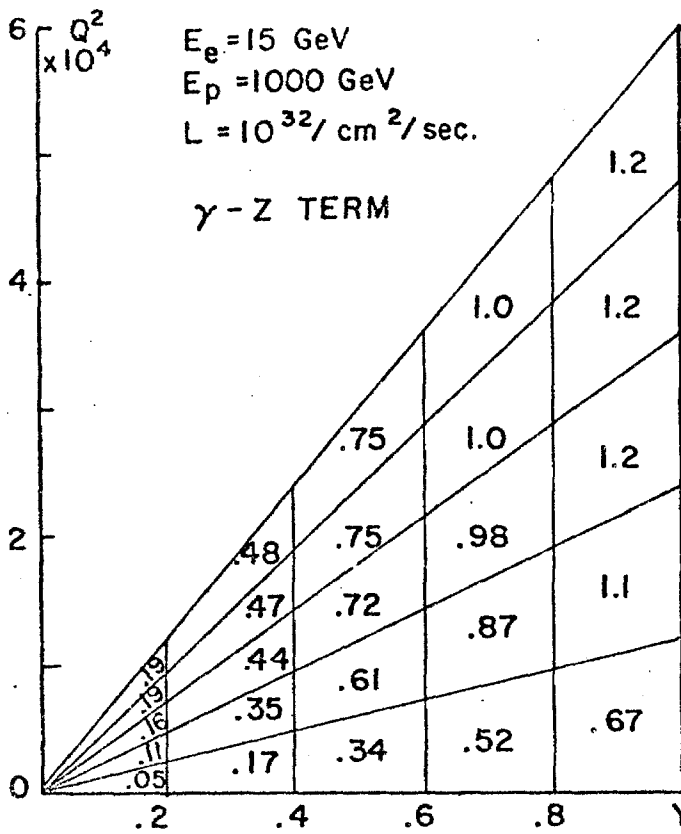


FIG. 3a

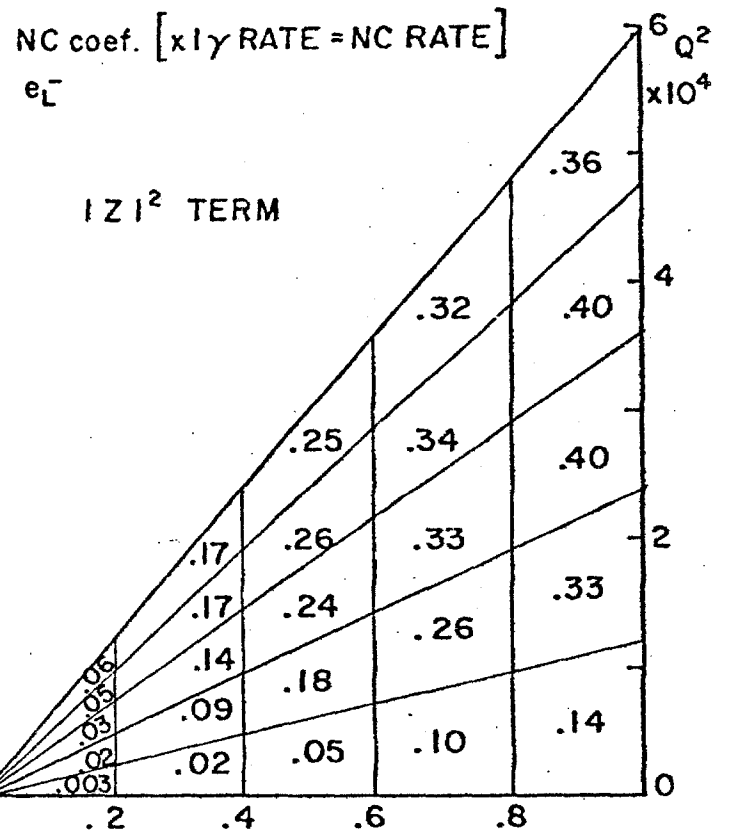


FIG. 3b

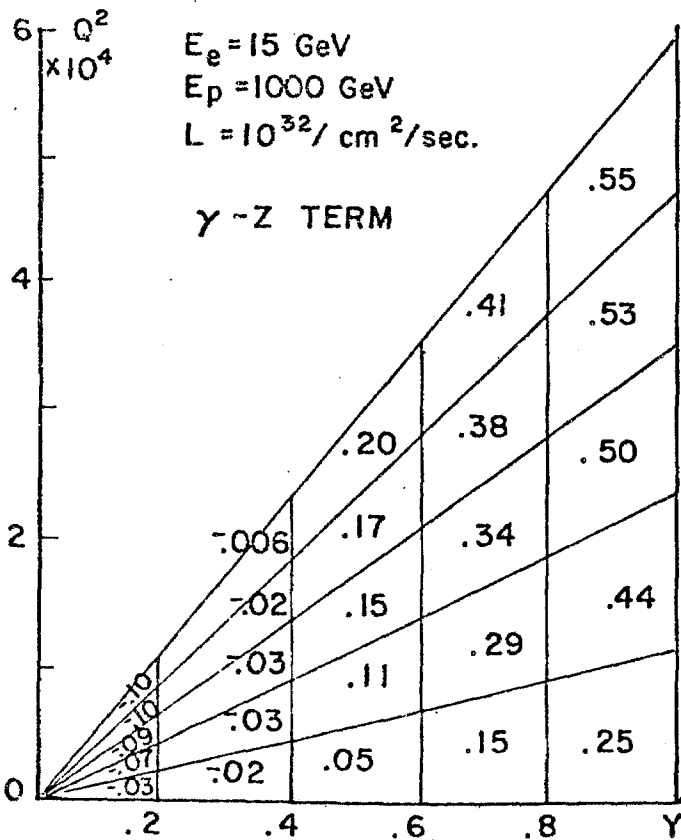


FIG. 3c

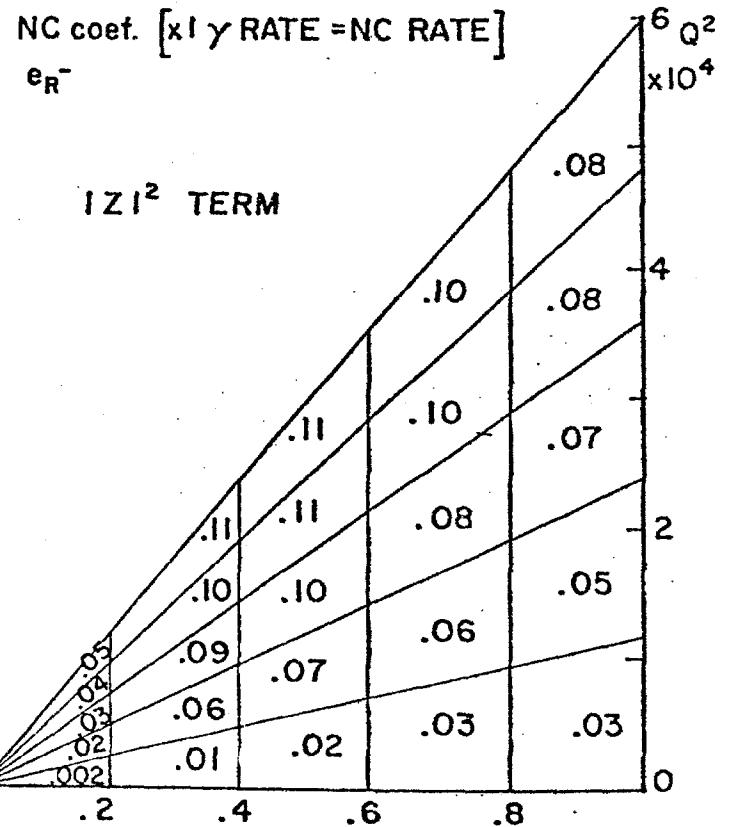


FIG. 3d

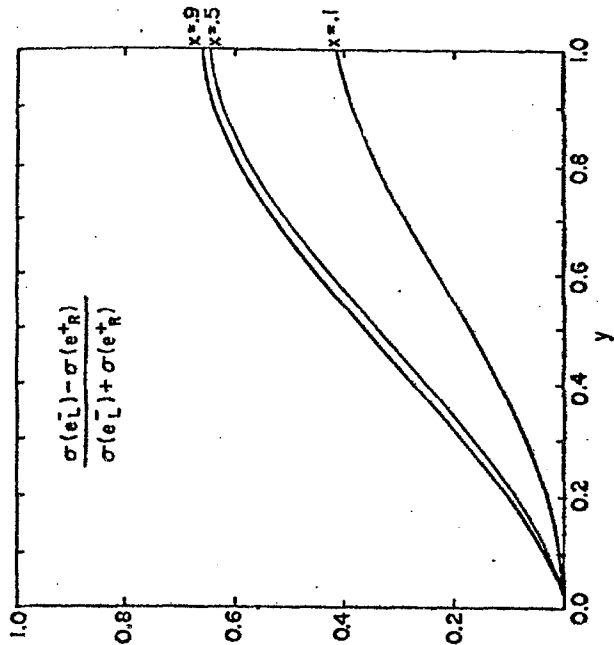


FIG. 4c

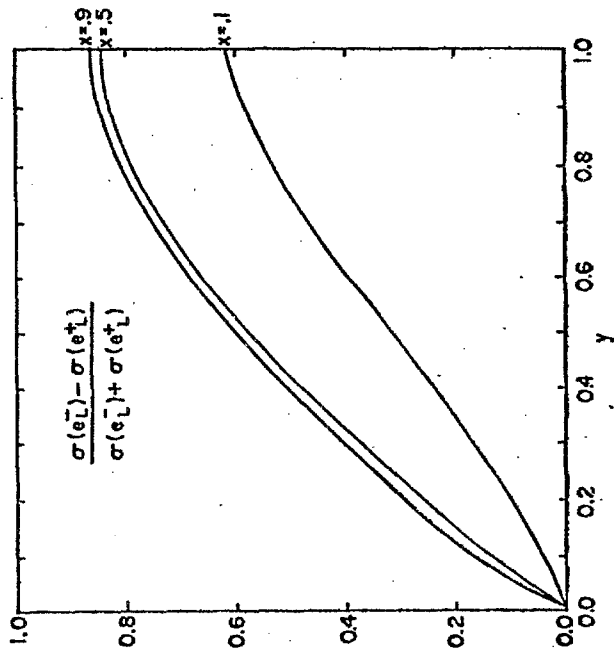


FIG. 4b

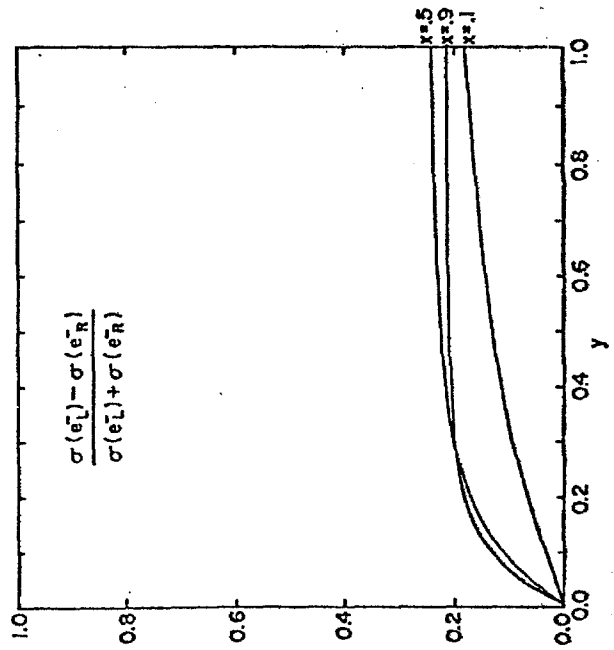
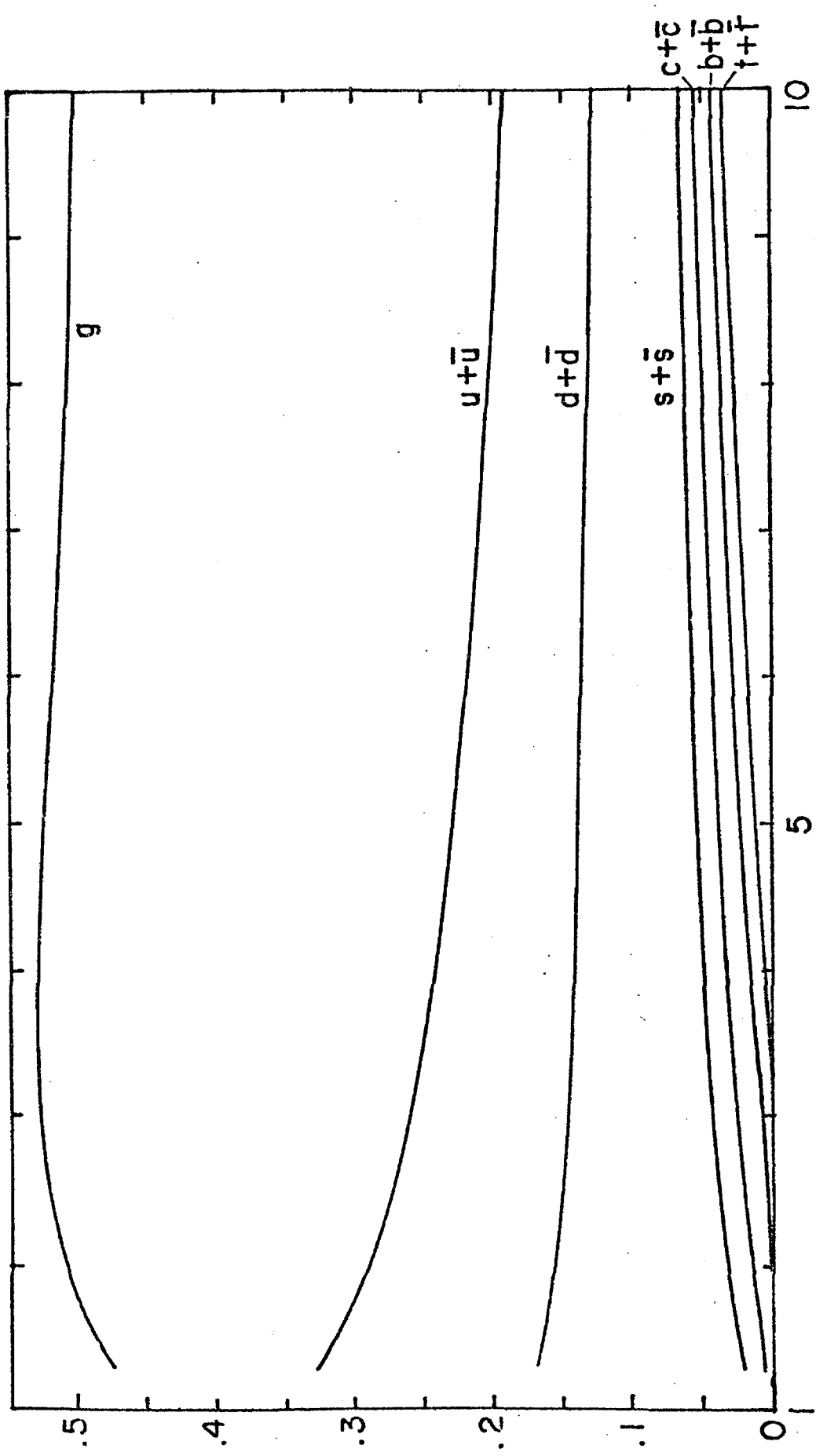


FIG. 4a

PARTON MOMENTUM FRACTION DISTRIBUTION



$$t = \frac{1}{2} \ln \frac{Q^2}{A^2}$$

FIG. 5

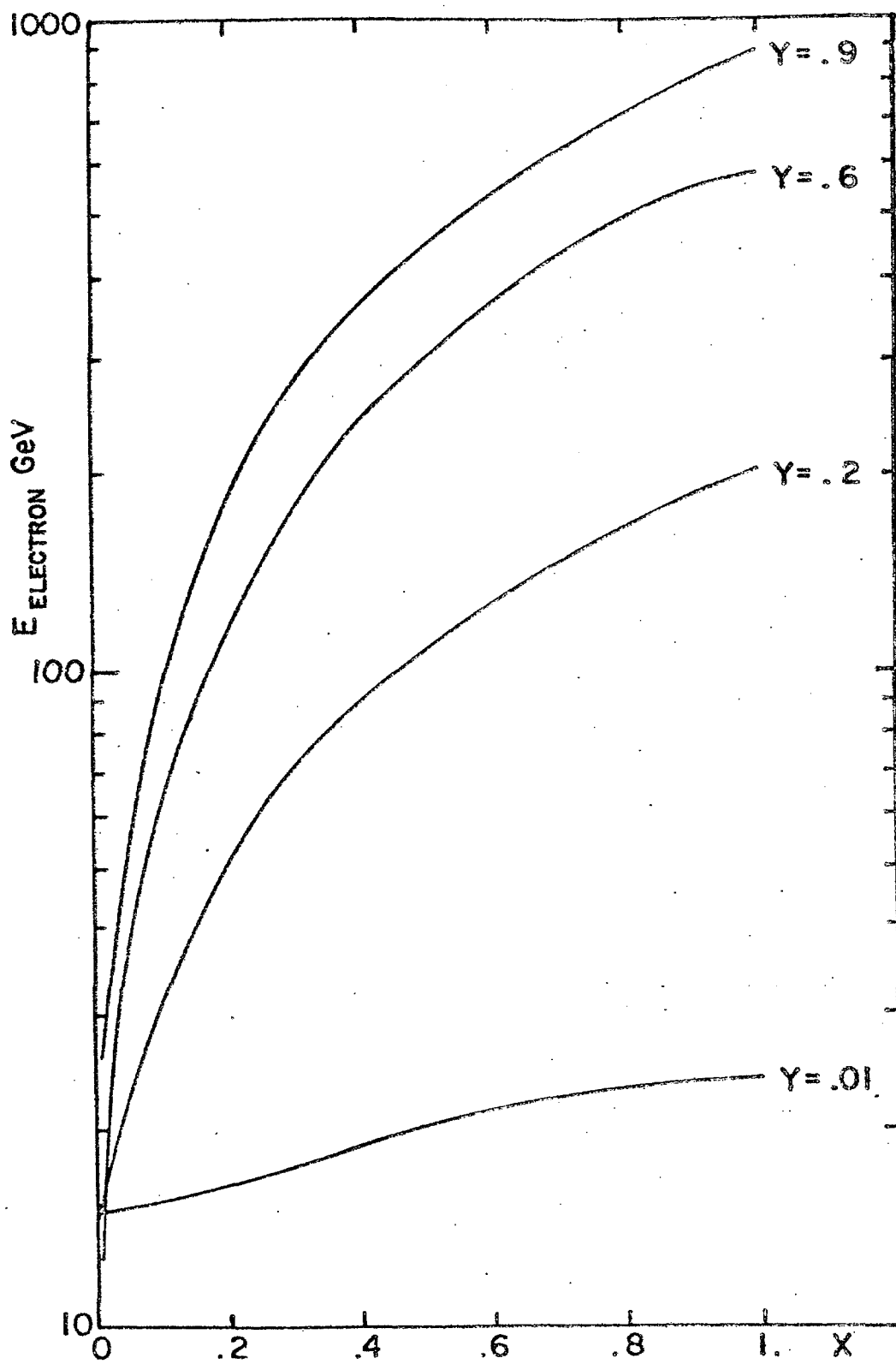
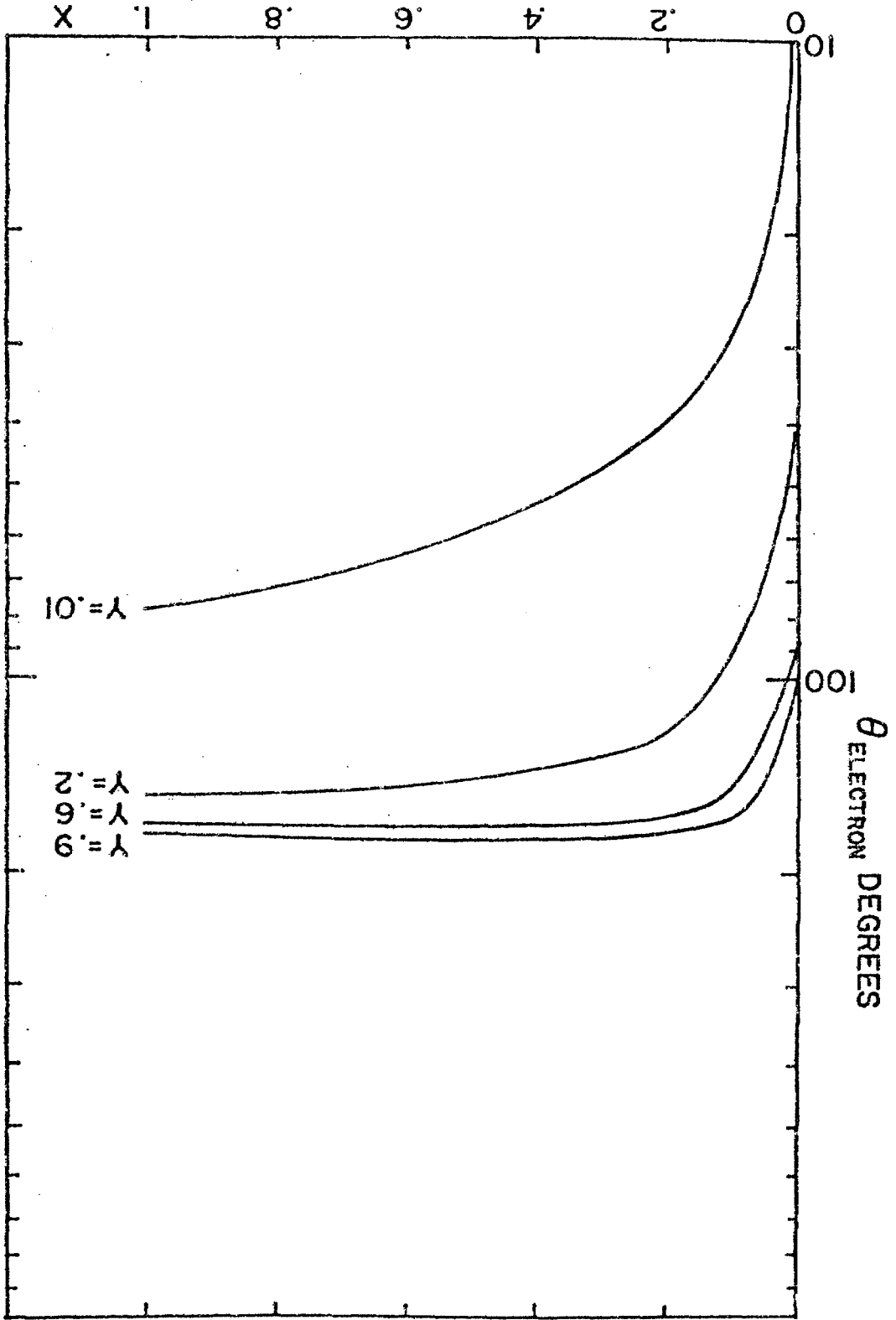


FIG. 6a

FIG. 6b



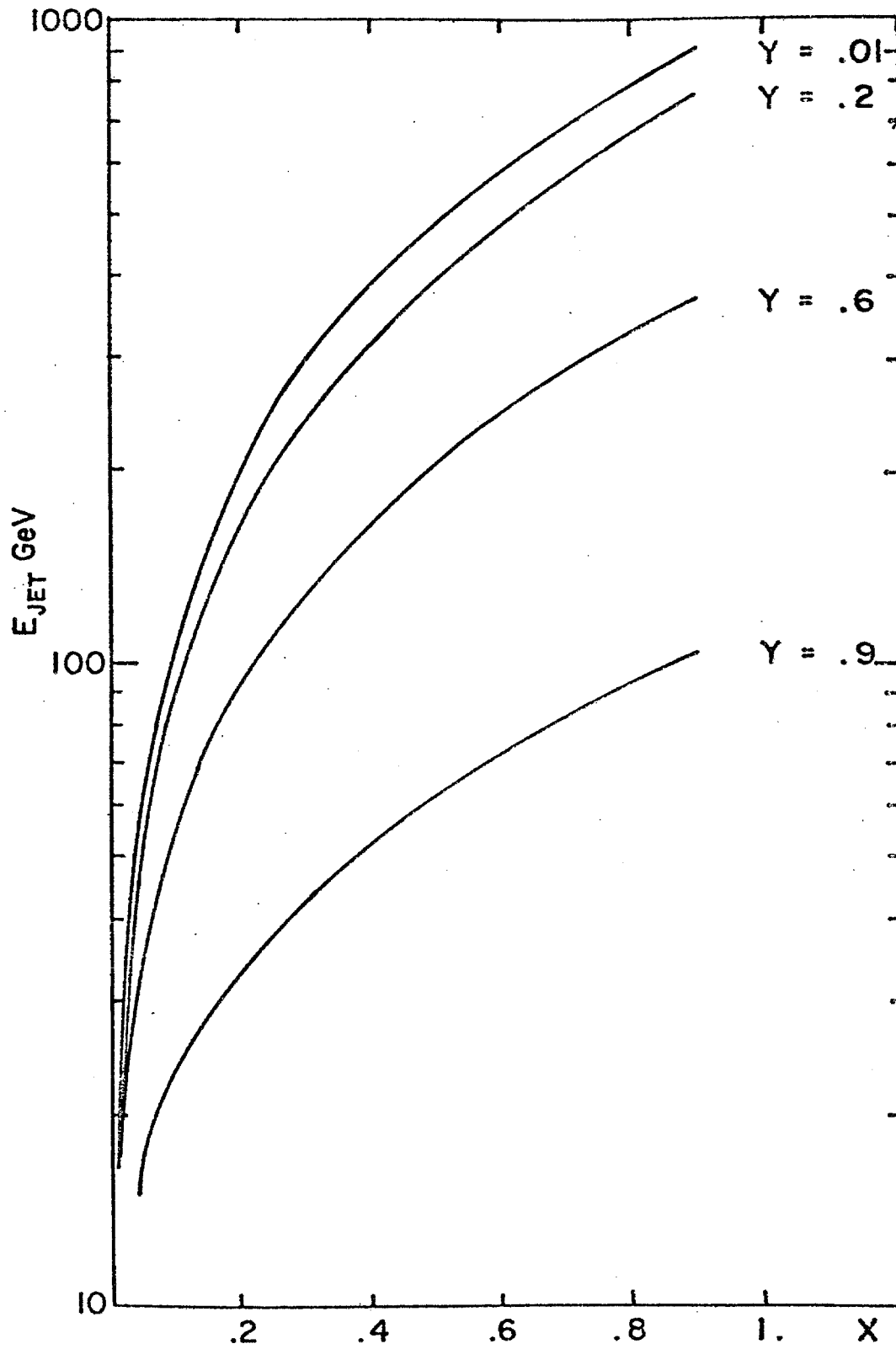


FIG. 6c

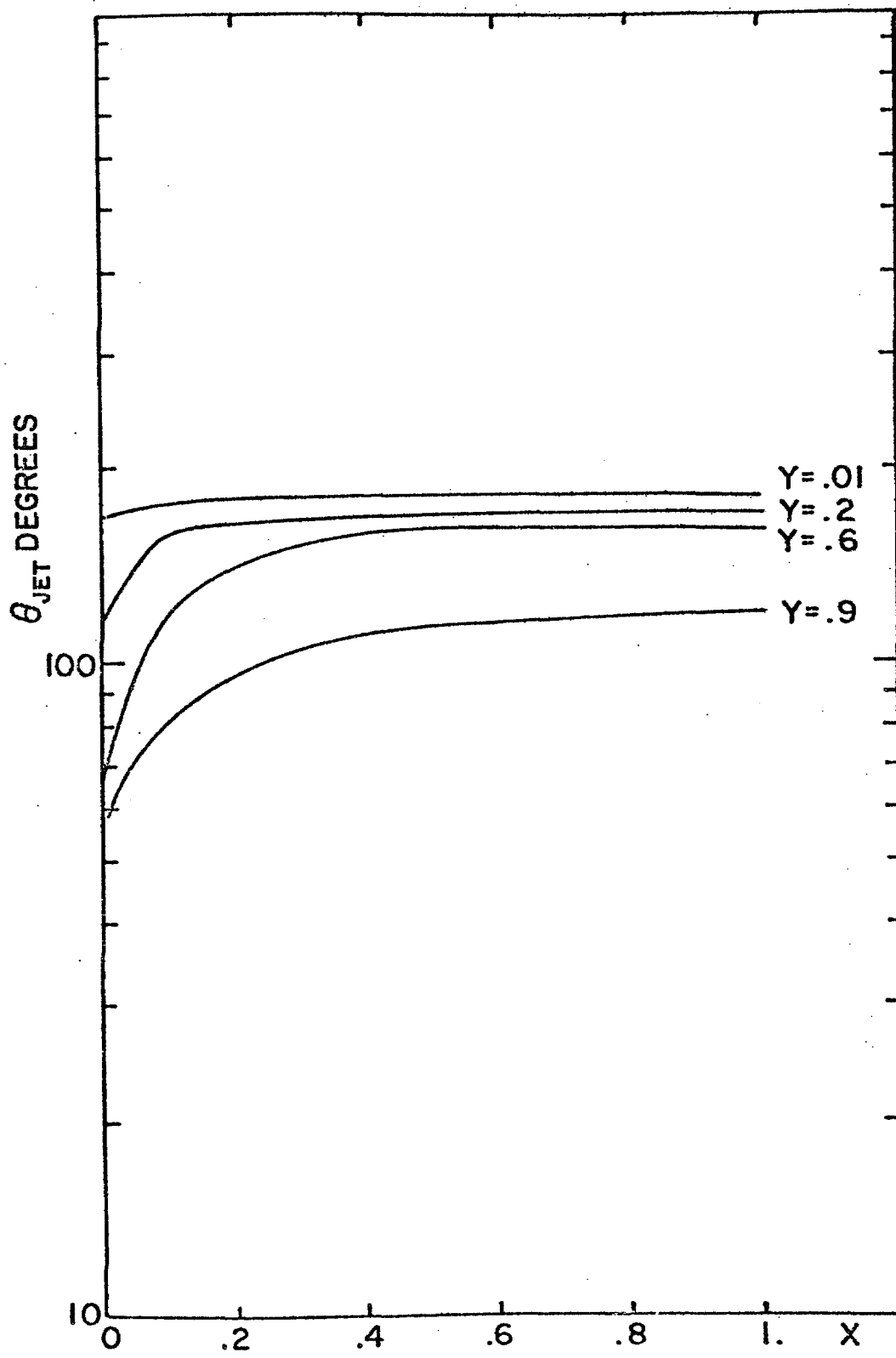


FIG. 6d

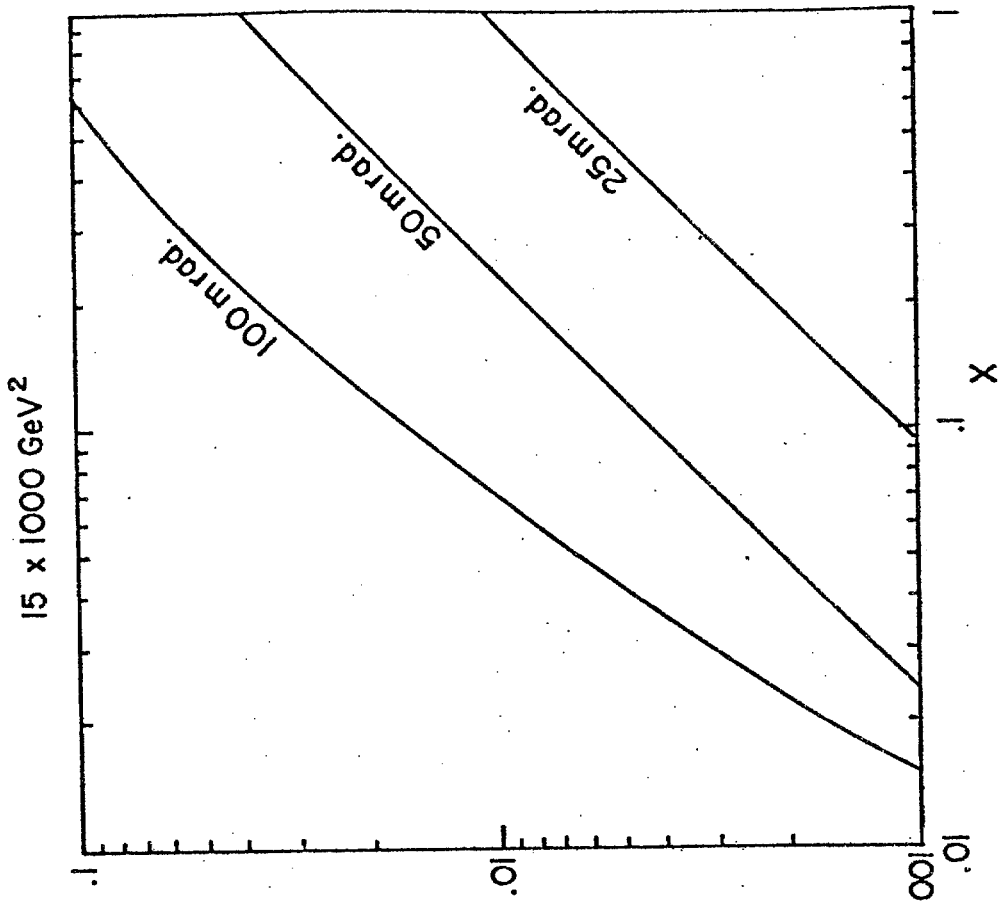


FIG. 7b

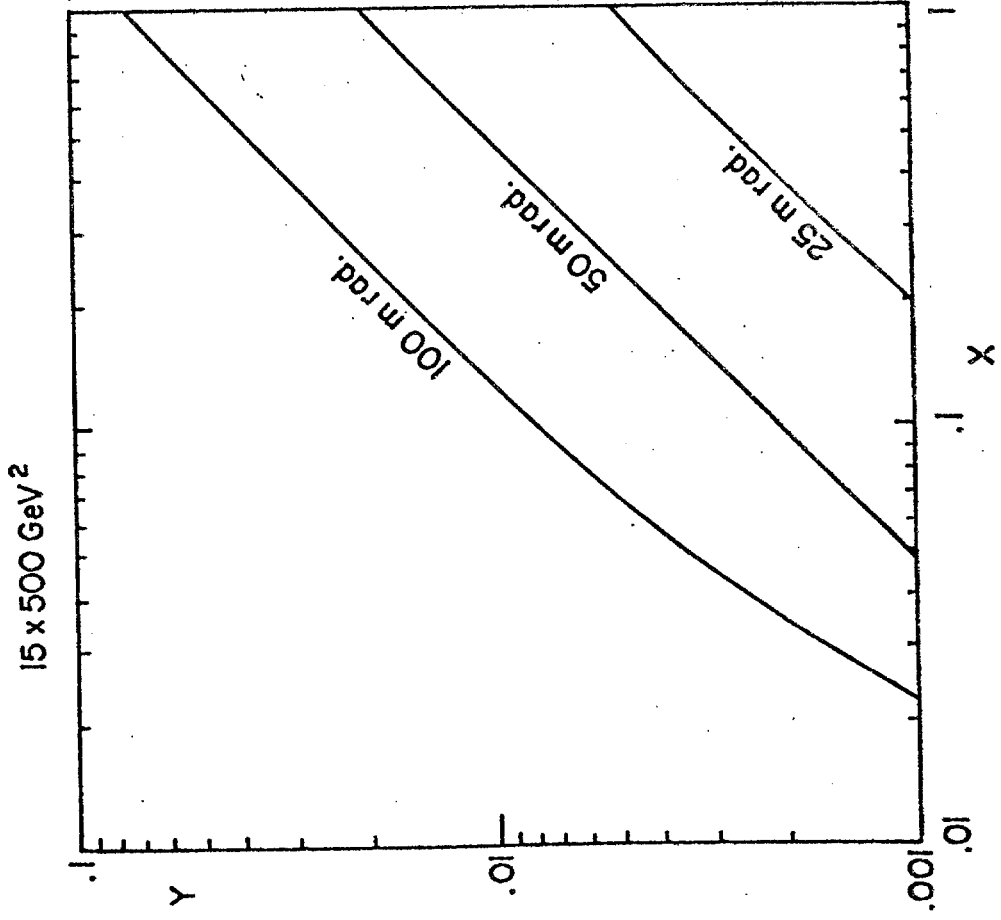


FIG. 7a

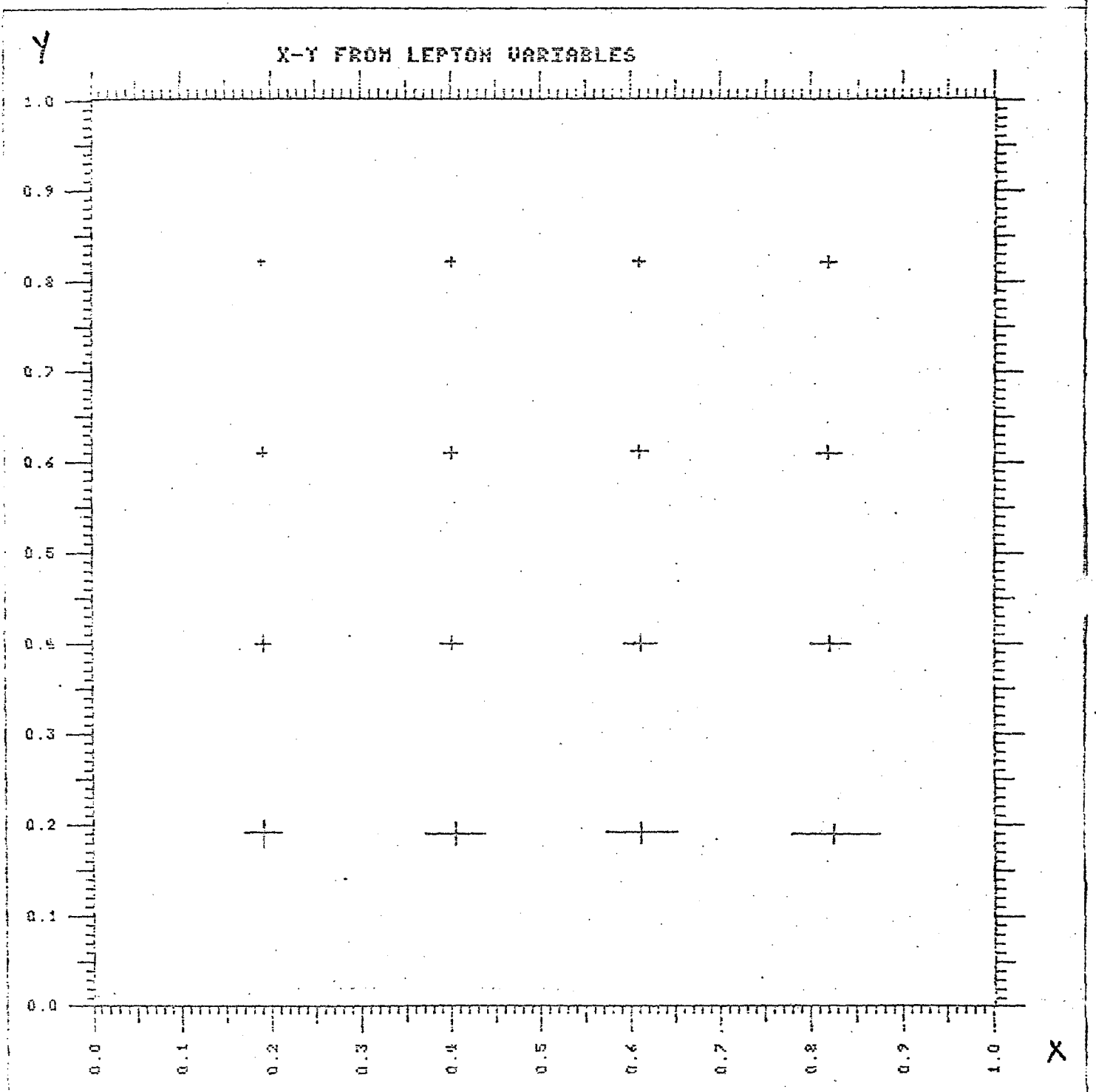


FIG. 8a

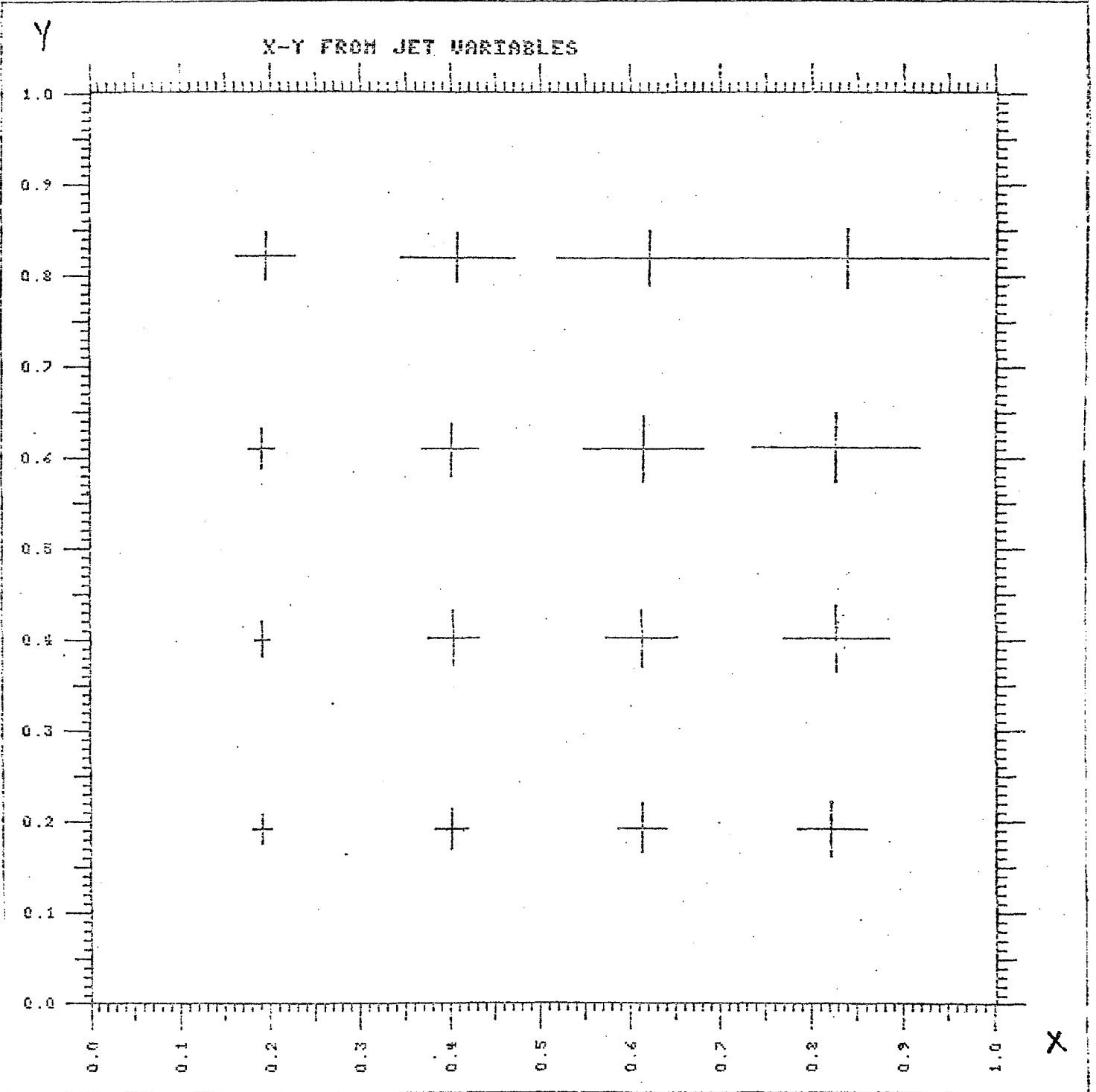


FIG. 8b

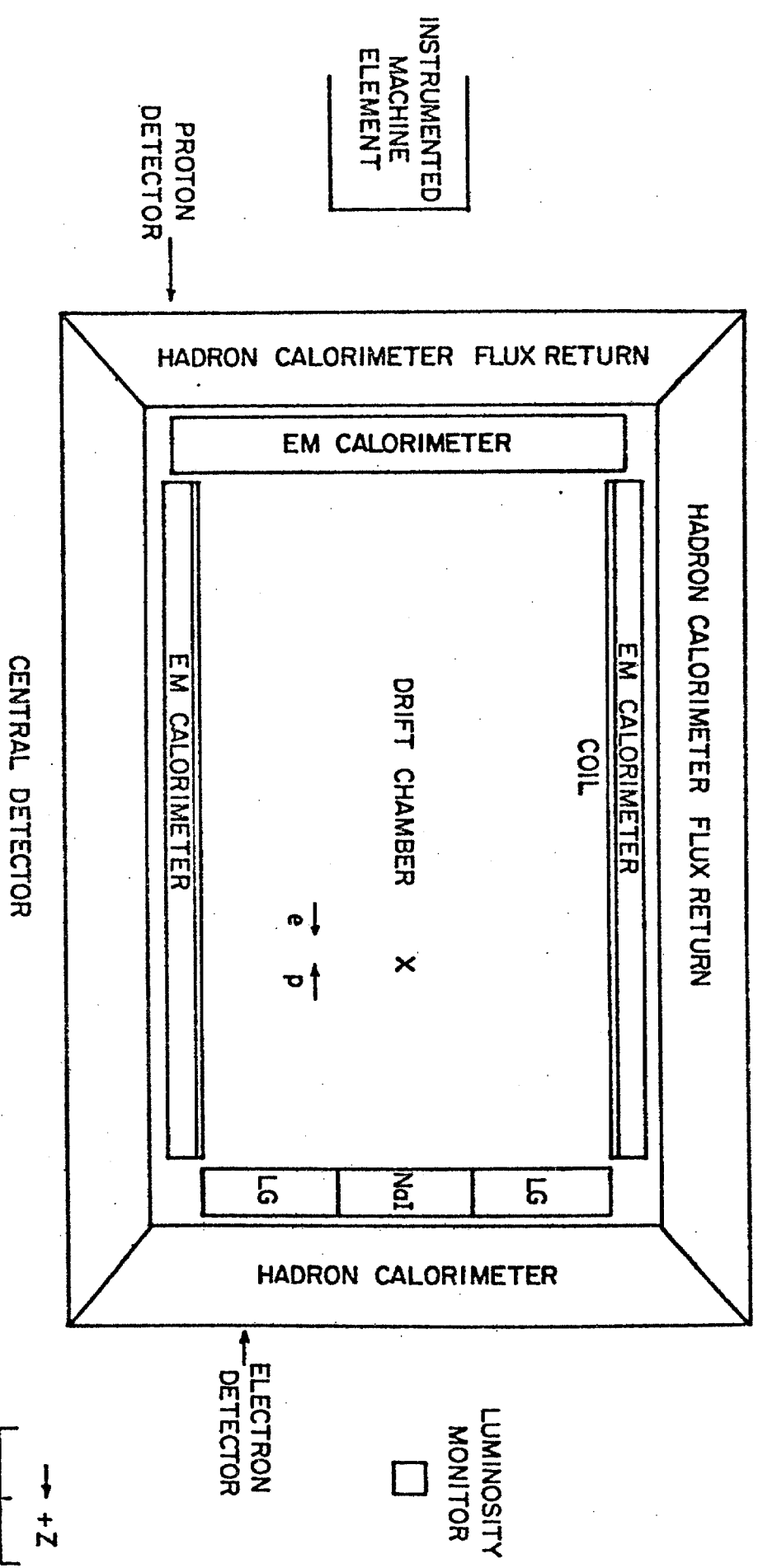


FIG. 9

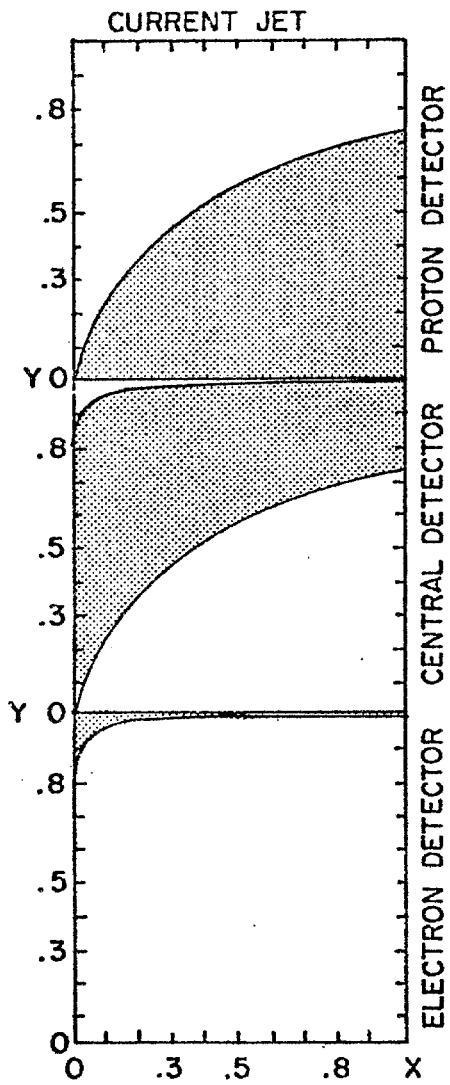


FIG. 10a

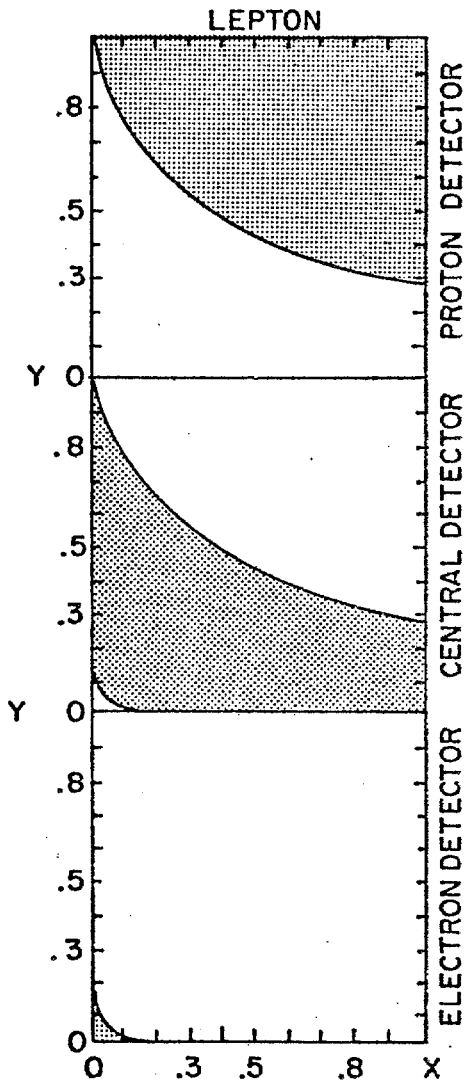


FIG. 10b

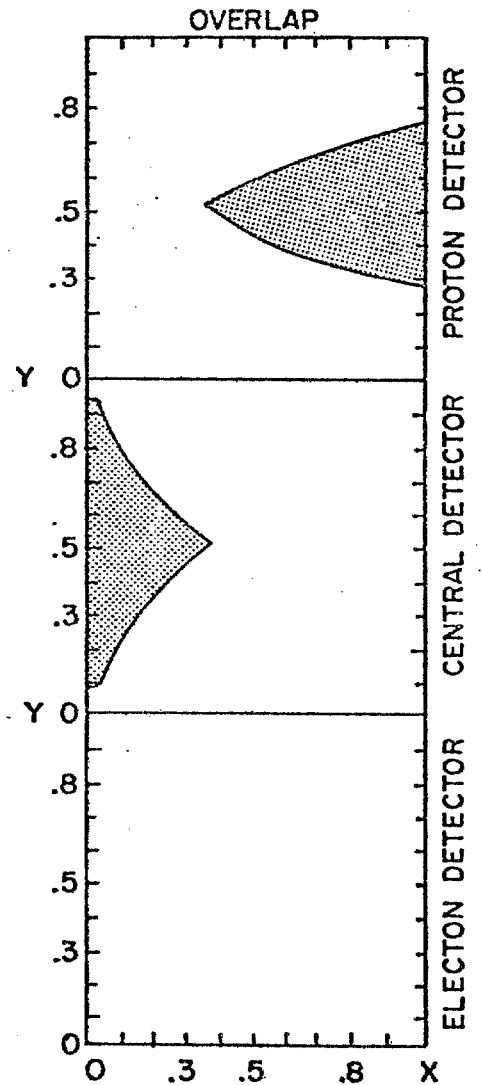
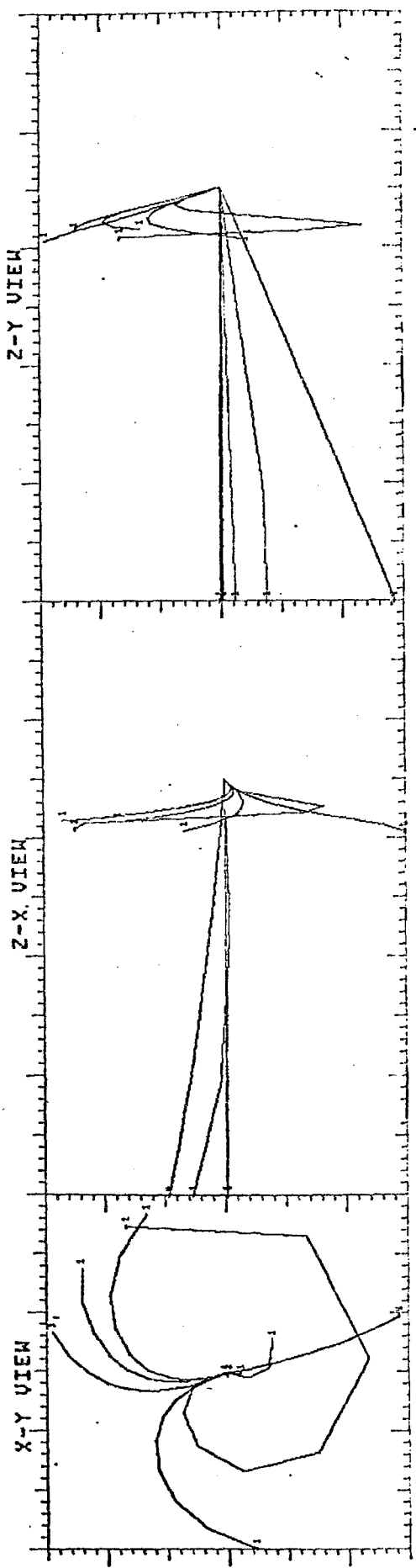


FIG. 10c

X	Y	EL	EC	ET	THL	THC	PHI
0.09	0.78	79.20	32.10	903.60	157.00	105.20	103.24



X	Y	EL	EC	ET	THL	THC	PHI
0.14	0.64	97.90	60.20	856.80	153.20	132.60	347.90

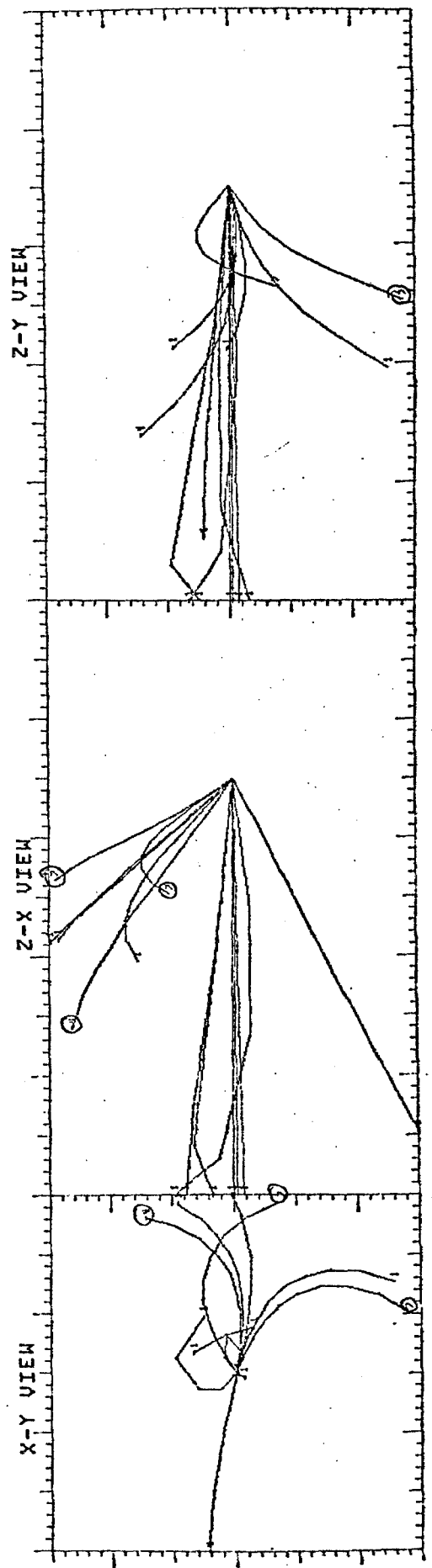


FIG. 11

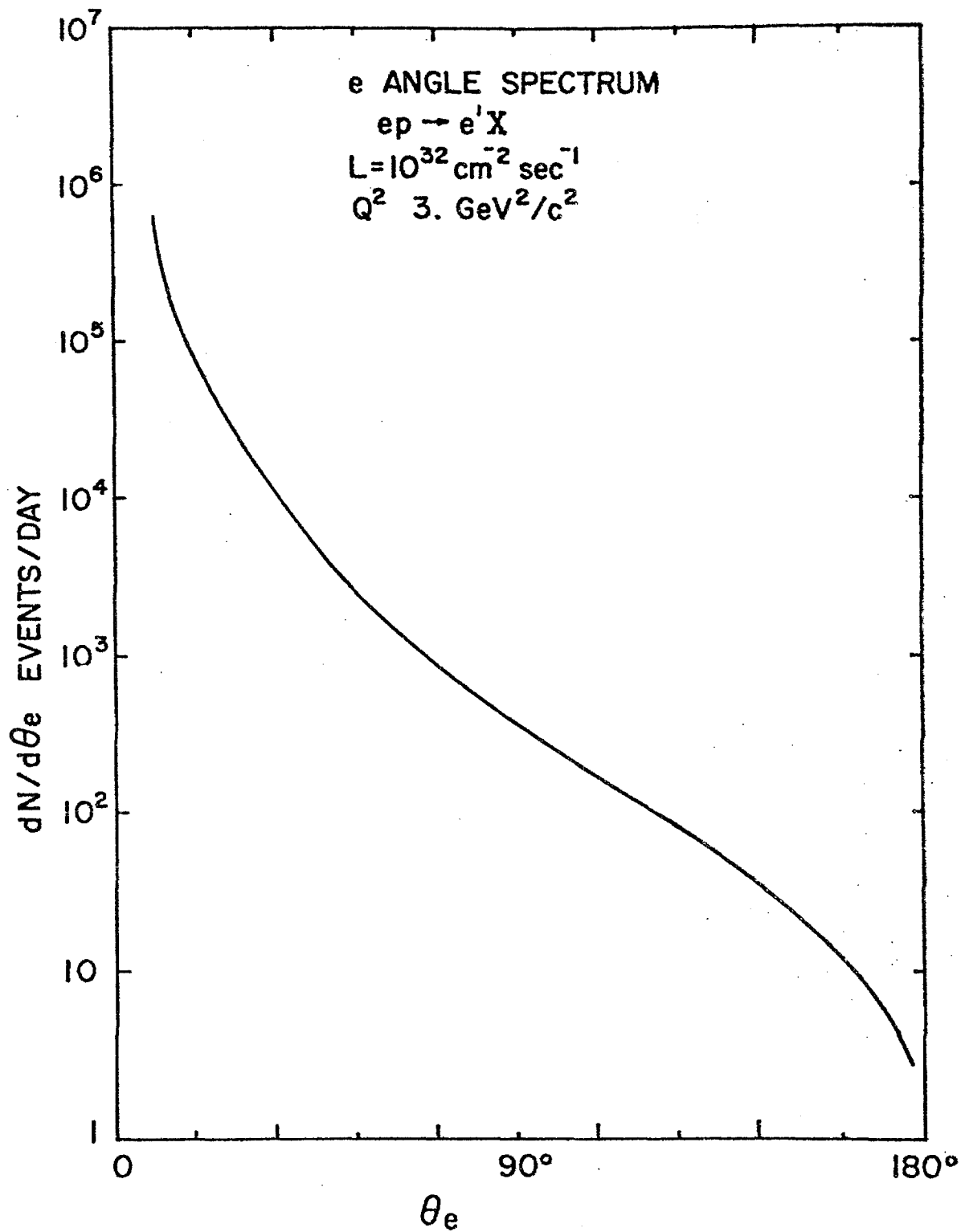


FIG. 12

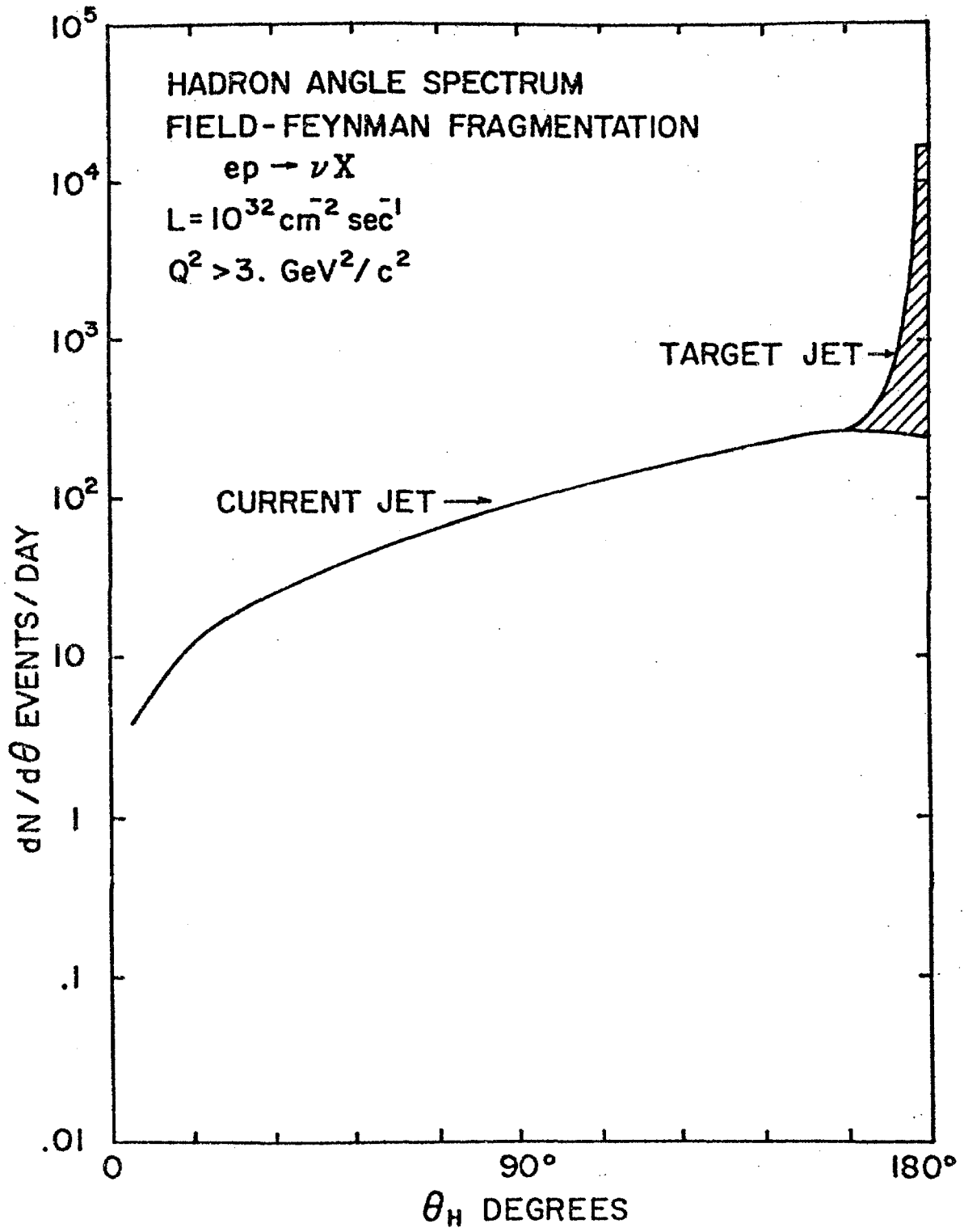


FIG. 13

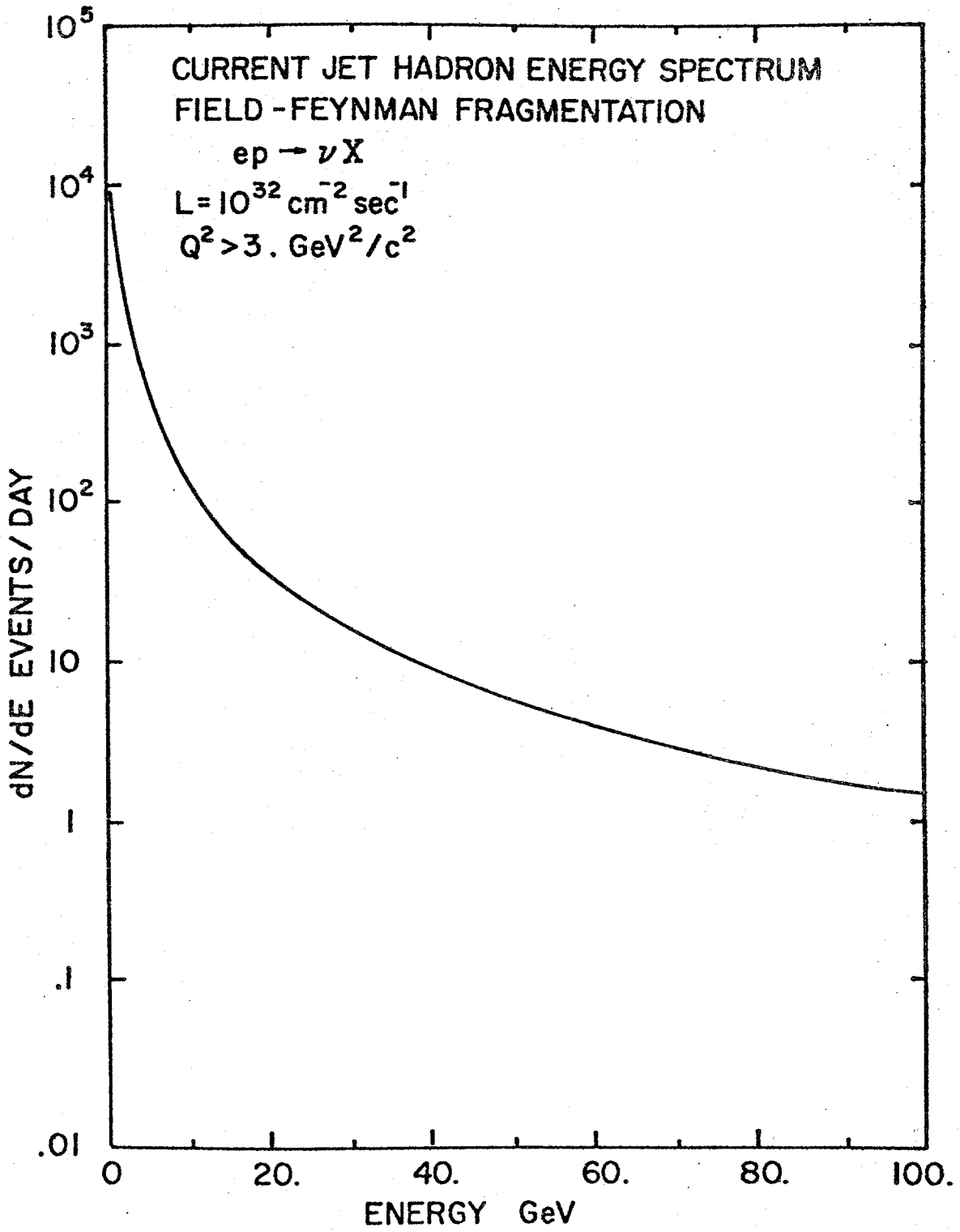


FIG. 14

VIEW OF 16 ELECTROMAGNETIC
CALORIMETER MODULES

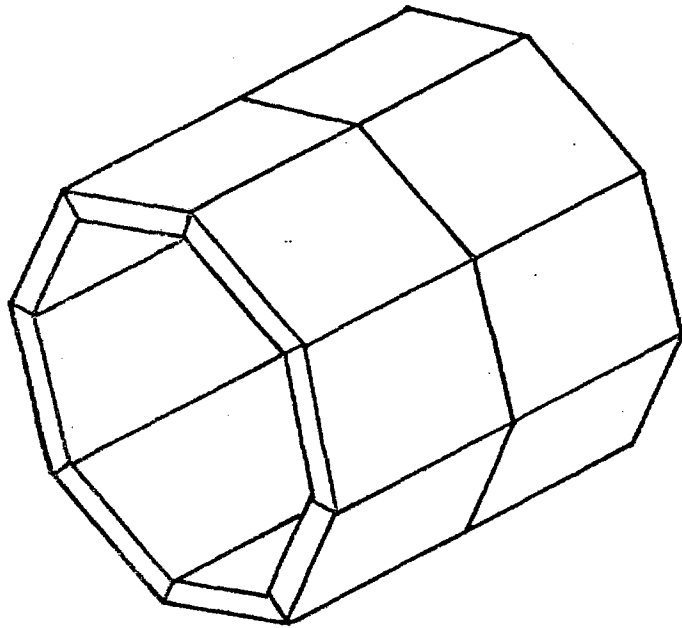
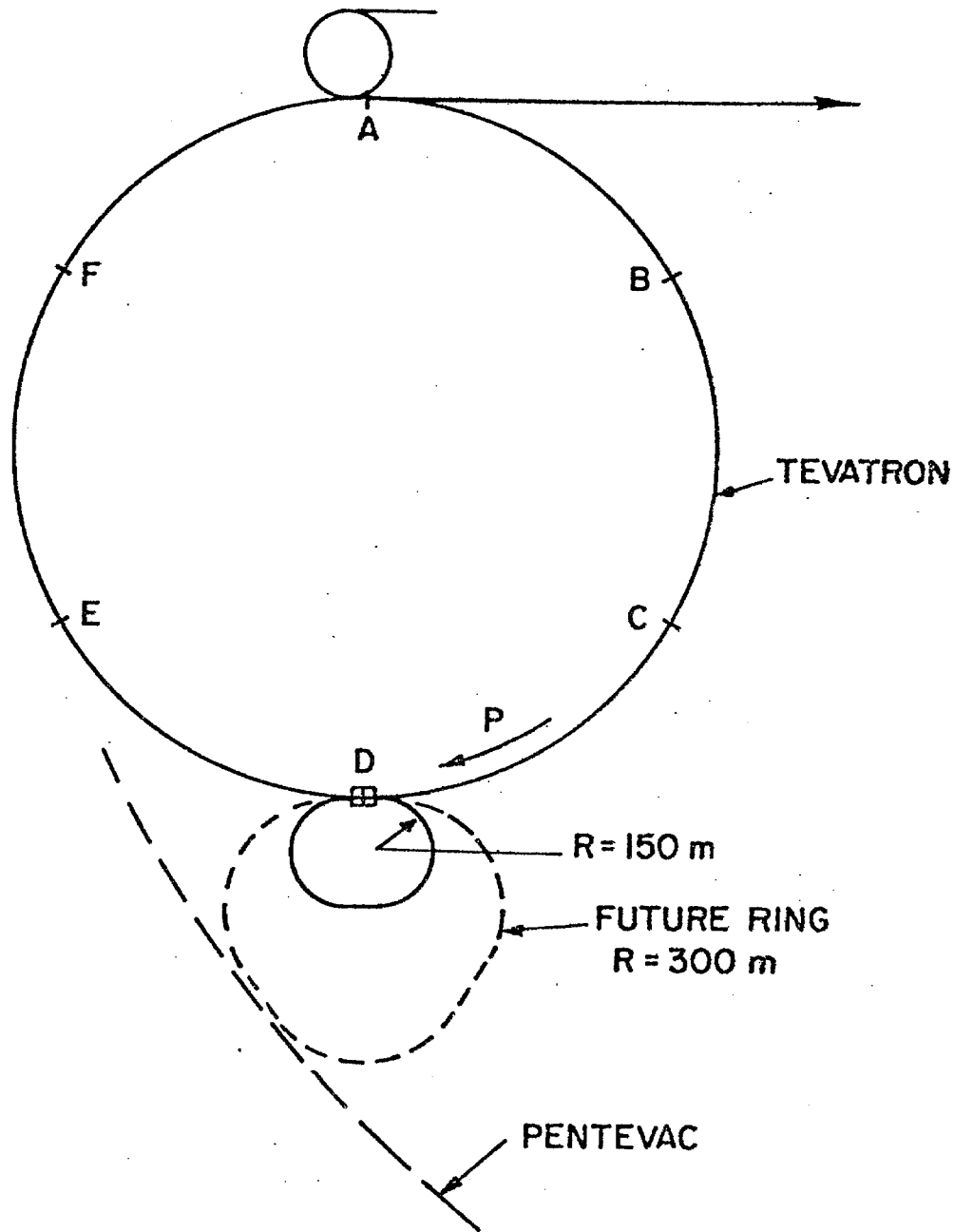


FIG. 15

FIG. 16



The electron storage ring.

A second ring of about 300 m average bending radius is indicated by the dotted lines to allow for running at a higher electron energy, 20-25 GeV, for collisions with the 1 TeV protons in the Tevatron. It might eventually turn out to be tangent to the Pentevac should such a device be constructed. This would then allow for, say, 25 GeV on 5 TeV ep collisions. The ultimate (well, the penultimate) might be to have a 75 GeV electron ring in the Pentevac tunnel, giving over 1 TeV in the c.m. system of 75 GeV/5 TeV ep collisions. If the 300 m ring were to be built, the first ring would be most useful as an injector into the second ring, as a device for polarizing the electrons, and as a part of the preparation of a positron ring.

T. D. Lee

Maybe I could make a theorist's statement. Let me put aside machine considerations. If you look at physics at large, we have both in the U.S. and in Western Europe several machines designed to discover Z^0 several times over. The proton facilities in the U. S. are quite unique, and we could take the rather modest step of putting in a 10-15 GeV electron ring to explore the ep physics we have heard about in the last two days. It is unique physics. There is almost no question that the world is made of quarks and leptons. We can collide quarks on quarks, leptons on leptons, and quarks on leptons. Nothing more needs to be said. The question is when can we explore the quarks on leptons region of physics, and over what parameters. I am happy to see that this conference has covered all the physics you can do with ep. If you like the spectacular, you can find if quarks and leptons have structure, or you can simply study proton structure, or, if you are a QCD enthusiast, you can test the validity of the theory. Listening to these talks here makes it absolutely clear that ep physics is not duplicated by p-p or \bar{p} -p, not duplicated by e^+e^- , and the converse is also true. Therefore, with this scenario, we should ask ourselves if we should base our program on running on the second line to the European machines, to discover the Z^0 several times behind everybody else. To concentrate single-

mindedly on \bar{p} -p or e^+e^- is a mistake. Many years from now we will look back, and if because of our prejudice, if because of narrow mindedness, or if because of our incompetence, we forsake this relatively simple step which opens the door to a huge amount of physics, then we will regret it. We will not have done justice to ourselves or our community.

Chris Llewellyn Smith

Theoretical Issues in ep

May 3, 1980

1. Introduction

I will limit the discussion to three possible machines and discuss the issues that they can address. One usually starts with a list of issues chosen carefully to put ep in the best possible light, I will not do this here.

The three machines are (see Fig. 1):

1.	20 x 400	$s = 32000$	ISABELLE
2.	15 x 1000	60000	FERMILAB
3.	30 x 800	96000	HERA

Many items are taken from the theory section of the HERA report.

A large new energy region is opened up (Fig. 3), lines of 10 events/day are shown. In Fig. 4 the number of events per day above a certain Q^2 are given for neutral currents. One event/day for $Q^2 > s/3$, 10 events/day for $Q^2 > s/5$. This is very similar for charged currents as well (Fig. 5).

What can we do with these events?

2. Neutral Currents

First neutral currents, model $SU(2) \times U(1)$.

What about further gauge structure?

Can we test this in ep collider? Look at three possibilities:

1. Consider $[SU(2)]^n \times [U(1)]^m$ (Fig. 6).

It can be reduced at small Q^2 to the standard model, except for one extra term $\frac{G}{\sqrt{2}} c (J^{em})^2$. This term would not have been seen in neutrino scattering because the neutrino is neutral. Nor would it have been seen in the SLAC parity violation experiment with polarized electrons because it conserves parity. It would show up in Bhabha scattering at PETRA, it did not which limits $c < 0.15$. Not very stringent constraint.

Of course at high Q^2 more vector bosons will show up. To ensure that the coupling at low Q^2 is standard, at least one of the Z^0 must have a mass lower than the Z^0 of the standard model, i.e. lower than 90 GeV!

2. Model with left-right symmetry.

Left and right-handed W and Z have different masses.

Because the standard model works well, the left-handed sector will imitate the standard model. The right-handed sector must have masses > 0 (200 GeV). Can we see this in ep?

This assumes standard couplings to quarks. If for example the right-handed W's want to turn only light quarks into heavy quarks (for example $d \rightarrow t$) then they could be much lighter. What do we see? Right-handed neutrinos will exist as well as right-handed currents. Extra Z's will exist.

3. SU(3) x U(1) Fig. 7). Quarks are in triplets.

There is no t quark necessary. Mixing will occur and strangeness changing currents must be avoided. Georgi and Pais have shown how to do this. In this model, there are flavor changing currents in b decay. If there is no top quark one can find out by studying b decay. Leptons are put in triplets as are the quarks. Octet of W's must exist. For example one can have $e + u \rightarrow \nu' + b$ where ν' is a new sort of neutrino. If $(\nu') = 0$, then to avoid conflict with μ decay and β -decay rates, the new W's must have masses $m_W > 240$ GeV. If $m(\nu') = 5$ GeV, the new W could be light and the reaction $eu \rightarrow \nu'b$ becomes as strong as normal reactions.

Another example: $e_R^- + q \rightarrow \tau^- + q$, is flavor changing leptonic current.

General lessons:

1. Standard currents couple to more than one Z and W. Cannot be seen at low energies. They could have non-conventional masses.
2. If extra Z's and W's couple light quarks to heavy quarks with mass > 10 GeV, then we would not have seen this. These Z's and W's could be light.
3. Exotic W's and Z's that couple light quarks to light quarks must be heavy $m > 0$ (200 GeV) to maintain low energy phenomenology.
4. The electron couples to a new neutrino ν' . If $m(\nu') = 0$ then $m(W) > 0$ (200 GeV). For $m(\nu')$ large, $m(W)$ can be smaller.

5. Flavor changing leptonic currents can occur.
6. Note that ep can "see" W's and Z's that are heavier than \sqrt{s} by their propagator effects.

3. Charged Currents (Fig. 8)

For rates, see Figs. 9 and 10. Rates per day are good, note suppressed zero in Fig. 10. When we go from e^- to e^+ the rate drops somewhat because we scatter off d quarks instead of u quarks and there are fewer of them, and because of the usual helicity factors.

How well can we see a standard W? See Fig. 12. W is clearly detectable for $m(W) \sim 300-500$ GeV depending upon which of the three machines are considered. Resolution $\Delta m = 5\%$. Figure 8 summarizes resolution in Q^2 good for $Q^2 \leq s/4$ and sensitivity to $m(W)$ up to $m_W \leq 1.6 \sqrt{s}$. If there are two W's it is hard to tell with ep. ep is in the spacelike region and the two poles are in the timelike region. One can mock up a single pole with the sum of two poles. But suppose we already know that one W exists, say at 70 GeV, but it does not have the right coupling to reproduce β decay. Can we tell whether there is a heavier W? We can tell that $m(W_2) \neq \infty$ for $m_2 \leq 1.5 \sqrt{s}$ or 270-470 depending upon which of three machines are considered.

New quarks, leptons, currents (lower part of Fig. 8). Up to what mass of W are we sensitive for light leptons and quarks? Rates are given on top of Fig. 13, sensitivity up to 500 GeV.

If $M_q \approx 5-10$ GeV and $m(W') = 78$ GeV, then table at bottom of Fig. 13 and Fig. 14 gives sensitivity to heavy leptons up to 160 GeV. Even if quark is 100 GeV and heavy neutrino is 50 GeV, we get 50 events/day!

If new neutrino is massless and quark is 150 GeV, we get 10 events/day.

ep is sensitive to fantastic masses even if $m(W')$ is larger than 70 GeV (see Fig. 15).

Can we see this? Use right-handed electrons, this is absolutely fundamental! Signatures in Fig. 17. The new heavy quark and heavy lepton will decay through their own new current to the lightest lepton or quark to which it couples. Those in turn will be either stable or decay by mixing with the light quarks. There will be a current jet consisting of a heavy quark at a large angle. The heavy lepton will decay into an electron, a light quark and a heavy quark for example (if lightest heavy quark is lighter than the lightest heavy lepton). Signature is spectacular.

4. Back to Neutral Currents

What are the signatures?

1. Parity violation

2. Apparent C violation: $\sigma(e_L^-) \neq \sigma(e_L^+)$
 $\sigma(e_R^-) \neq \sigma(e_R^+)$.

Two photon exchange gives this too but it has very different characteristics.

3. γ distribution is different: it has an F_3 type term due to V-A interference.

All this has been extensively studied and will not be repeated. But it is clear that one needs electrons and positrons of both polarizations.

Rates, see Fig. 19 and 20. Figure 21 gives dependence of $\sigma(e_L^-)/\sigma(e_R^-)$ on $\sin^2\theta_w$, it can be determined with an uncertainty $\Delta(\sin^2\theta_w) \sim 0.01$ and $\Delta m(Z) \sim 5-10$ GeV from Q^2 dependence independently. If two Z's exist and one is 50 GeV, then ep is sensitive to second Z if $m(Z_2) < 100-200$ GeV depending upon which of three machines.

For left-right symmetric models, we get a better limit on m_R , see Fig. 22. Solid lines are standard. The lightest extra Z allowed by the SLAC parity violation experiment has $m(Z_R) = 224$ GeV. It gives the dashed lines. Figure 23 gives same information. Maybe can be done for $m(Z_R) = 400$ GeV.

5. Production of Free W's and Z's

Cross sections are pathetic (small), this is not the way to discover them.

6. Strong Interactions and QCD

Two parts: 1. Structure functions,

2. Details of the final state.

For neutral current easy by presence of electron in the final state, but weak effects are small with respect to the electromagnetic effects, see Fig. 25.

Charged current have missing neutrino but are still easy to detect. Use special expression for y , see bottom of Fig. 25. Resolutions in x and y are given in Fig. 26.

Figure 27 gives the reconstruction characteristics from hadron measurements only.

Figure 29 gives the scaling violations as function of $Q^2 = 2, 10, 100, 1000, 10^4$. Lots of action near $Q^2 = 2, 10, 100$, less beyond. Sometimes people react to this by saying that it is a waste to go to high Q^2 and that one is better off at low Q^2 . This of course assumes the validity of QCD and that is what we are after to check! We have got to see the scaling violations stop at high Q^2 . Large Q^2 will also remove higher twists finally and enable to distinguish between logarithmic and power law scaling violations, see Fig. 30.

σ_L/σ_T is hard but interesting to measure.

Deuterium in the machine would be nice.

Now second part: details of the final state.

At high s , 2 jet events become interesting, see Fig. 32. Look at rapidity plot where the removal of the stuck quark leaves a hole. Need much more than 2 units of rapidity (correlations are over 2 units of rapidity), so large Q^2 and large s . Look at particle ratios and search for large distance correlations in them.

Fragmentation functions can be measured with the identity of the parent known: $e^-u \rightarrow \nu d$, contrary to e^+e^- : Three jet events will become manifest. The non-perturbation background will be small with respect to QCD effects at these high Q^2 .

Contrary to e^+e^- case, in ep neutral current case one knows the current quark axis by measuring the electron. So one knows where the current jet should have gone if it were a 2 jet event. Figure 34 gives an event with 3 jets: an extra gluon jet is present.

7. Photoproduction

Spectrum of Weissacker-Williams photons.

Integrate over their spectrum to jet $L(\gamma p) = 10\%$ of $L(ep)$ for untagged and $= 1\%$ of $L(ep)$ for tagged photons.

Gives millions of events/day. Look at soft hadronic physics: σ_T as function of s , lots of J/ψ produced etc. (see Fig. 37).

Large P_T processes can lead to 3 and 4 jet events owing to the point structure of the photon. The photon structure function antiscales with Q^2 : they increase with $\ln Q^2$ which cancels out the extra power of α_s in the 4 jet event with respect to the 3 jet events. So both should occur equally and have the same scaling behavior. It will lead to $P_T \sim 10-15$ GeV/c! See Figs. 38 and 39.

8. Production of Heavy Quarks

At high Q^2 and low x , there will be democracy among the different flavors. What are its consequences?

Conclusion is that ep is not comparable to e^+e^- for production of heavy quarks out of the sea; you run out of rate at $m_q \approx 20-40$ GeV/c². See table at bottom of p. 40.

But QCD has a lot to say about the dynamics of their production; it is a rather interesting set of detailed predictions.

9. Novel Phenomena

1. Higgs? Cannot be discovered

$$\sigma(\text{Higgs}) \sim G^2 \quad 1 \text{ event/day}$$

2. Technicolor schemes have things like Higgs with similarly small cross sections.

3. Exotic quarks: free quarks produced by high Q^2 impacts.

4. Quarks with $Q = 5/3$? They give big rise in F_2^{em} at small x - example $e^+u \rightarrow \bar{\nu} Q(5/3)$.

5. Integer charged quarks: disfavored now by recent measurements on eta decay. If you pass the Han-Nambu color threshold, they give a big rise in F_2 . Han-Nambu has charged gluons. As soon as Q^2 is large enough to excite them, a large increase in σ_L occurs.

6. Supersymmetry: particles of different spins in the same multiplets. Scalar quarks and spin 1/2 gluons could exist. Nobody knows at what energy scale they might come in, guess at same scale as weak interactions ~ 100 GeV. Scalar quarks give a large σ_L at small x . Spin 1/2 gluons will contribute to the momentum sum rule.

7. Leptoquarks must be listed; nothing to say.

8. Monopoles must be listed; nothing to say.

9. Substructure of quarks (see Fig. 44). Too many flavors, are they themselves composites?

ep very good for x-raying them—at large Q^2 , one can resolve substructure and excited quarks may be produced. Subquarks will lead to scaling violations at smallest x because their momentum distribution is softer than that of quarks.

Increasing Q^2 any further, one gets rescaling and the distribution shifts to small x .

Excited quark, consisting of 3 subquarks of spin $1/2$, may have spin $3/2$. This will give an enormous jump in σ_L . What happens at higher Q^2 depends upon the spin of the subquarks. If it is spin $1/2$, σ_L will go down again to 0. If some of them have spin 0 (and are charged) σ_L will stay up.

Toy model to show what may happen, see Fig. 45. If this is right, one may see substructure in quarks with a form factor characterized by a mass m up to $\sim 3/s$ or up to 1000 GeV. LEP e^+e^- machine would not see this: a value of 1 TeV would give a 10% change in the cross section at the top LEP energies. You would not necessarily know how to interpret this.

10. Summary

1. Proposed machines open up a huge new kinematic region
rates ~ 1 event/day for $Q^2 \gtrsim s/3$

10 events/day $Q^2 \gtrsim s/6$.

2. Weak interactions, charged currents:

sensitive to $M(W)$ to $O(1.6 \sqrt{s})$

for second W , about same: $O(1.5 \sqrt{s})$.

New W' up to $M(W') \sim O(\sqrt{s})$

new quarks and leptons up to $M \sim O(\sqrt{s}/2)$.

3. Weak interactions, neutral currents:

sensitive to one or more Z 's

right-handed currents

couplings.

4. Strong interactions:

test QCD

structure functions

fragmentation functions

multijet events

5. Photoproduction

all soft hadron physics

unique jets (large P_T structure)

6. Heavy quark production

laboratory for QCD dynamics

7. Novelties

exotic quarks

supersymmetry

subquarks (up to masses of $O(3\sqrt{s})$).

No Conclusions as this is a Workshop.

Tom Collins

If I may be so bold, I know what the detector will look like but I am not sure what the interaction region will look like, so the nature of this experiment is to a great extent, the process of bringing these two beams together. That's where the flexibility is, this is where the great game is. Bringing electrons and protons together is non-trivial; it is the hardest of the colliding beam things; as we have two beams that are very difficult in character.

Let me remind you of some of the jargon. A machine is a linear focusing device and any beam that can be described as an ellipse propagates through as an ellipse of changing shape but constant area. For our convenience we describe the machine by an ellipse which repeats when it goes around once. That ellipse becomes a stationary thing as it goes around and becomes a description of a multi-turn beam. Now we do not care which turn its on, but only the shape of the beam. There is no definition of the beam until we make it close.

The equation that describes the beam is as follows:

$$\text{Area} = \mathcal{K} = \frac{1}{\beta} (\eta^2 + (\beta \eta' + \alpha \eta)^2) .$$
 α describes the tilt. We want $\alpha = 0$ in the middle of our intersection region.

$$\epsilon = \frac{E^2}{\rho} \mathcal{K}$$

$\beta^{1/2}$ describes the maximum x extent of the beam. It is important because in order to get the luminosity up we want a small envelope for the beam, hence a small β .

I am going to design something that can be built today with absolutely no handwaving. That will give us a lowest level, an absolutely guaranteed level for the luminosity, and we will work our way up from there with clever ideas and things.

We start off with protons which for 1000 GeV protons is anticipated to have an emittance of 0.02π mm-mrad for an ellipse which covers about 95%. This emittance depends on the beam current as:

$$\epsilon = (10 n/E) \pi \quad \text{for } n \times 10^{13} \text{ p .}$$

The beam will have a momentum spread of 0.2-0.3 eV sec and come around with an rf frequency of 53.1 Mc or 1113 bunches, some of which are empty in the process of filling the machine (see Fig. 1).

Now we do not want that many bunches because the collisions occur every $1/2$ a wavelength which means we will have collision just upstream and downstream of the interaction region causing a background. So we coalesce these bunches into every third bucket. The way you do that is that while you turn off one rf, you turn on the other at $1/3$ the frequency and at the right voltage. This process

coalesces the bunches quite efficiently. In the process, the emittance goes up, because the momentum spread goes up. This makes the next collision 333 in. away and in that case we will have 6×10^{10} particles per bunch. Then $\epsilon = 1$ eV sec which means the length of the bunch is about 3.4 nsec; the interaction region will be half of that.

The electrons are a totally different story (see Fig. 2). We have an enormous handle on what we want the electrons to be, since we can make the size of the ring as large as we wish, and we can make the emittance whatever we like. I assumed the emittance to be about 5 times that for the protons ($\epsilon = 0.1 \pi$). Now the electrons come out in a flat ribbon which is bad for the luminosity because of non-linear effects, so we couple them intentionally to get a round beam. That implies that we want $\beta_e = \beta_p/5$ at the interaction region since we want both beams to be the same size when they hit each other.

(Here he gives an example of the flexibility of the electron ring . An important point he makes is that the polarizing elements should be separate from the rest of the machine.)

Luminosity

$$\mathcal{L} = \int^{\text{beam}} \text{current in beam 1} \times \text{density in beam 2}.$$

Since we want to tailor the electron beam to fit the proton beam, we will use the proton β and the electron current.

Both are the same size round beams so the integral is easy; we get (see Fig. 3):

$$\mathcal{L} = \frac{f_o}{3} \frac{h n_e}{4\pi\sigma^2} = 1.51 \times 10^{32} I_e/\beta_p \text{ cm}^2/\text{sec} .$$

Notice that in the process of putting the protons into 1/3 as many bunches, I have not changed the luminosity but I have cut the electron average current by three because I only had to fill 1/3 as many electron bunches. So I cut the power in that manner. We might be tempted to do more but I do not know how much I can increase that 6×10^{10} protons/bunch before stability problems arise.

How do we get the β down? I have redesigned the long straight section. It is my privilege to redesign the doubler on account of the fact that I designed it. I found it hard to get enough space because the real problem is to get the electrons in, put the protons back on their correct course, keep the synchrotron radiation out of the superconducting magnets and end up with some sort of β . I took the bull by the horns and said that the only way I would feel comfortable with the synchrotron radiation was to take out one of the superconducting magnets and replace it by three 20 kG normal magnets. (Synchrotron radiation \sim 1 kW. Magnets can stand only \sim 1 Watt.) This gives a deflection of about 2 in. before you hit the first superconducting magnet. I was not

worried about the quadrupoles where the beams are going straight through and the only radiation is scattered radiation, though they will still have to be protected. Then I ran out of space. But I came up with a solution shown in Fig. 4b. There is a much longer string of dipoles on each side and the three warm magnets. What do you do to find a solution? Well you must make the ellipses match up on either side otherwise you have to go back to the problem of closing the beam, and you find that you make the beam bigger and the doubler does not like that. The solution introduces two rather large quads 180 in. long, at 25.4 kG/in. For the "doubler" we built a three shell quad originally at 25 kG/in. but it was more practical to use two shell quads at the time. So I am totally certain we can build these quads. Then I end up with 750 in. on either side of the center. Figure 4c shows the β function; the little squiggle shows how powerful the two quads are. This solution has $\alpha = 0$, a momentum vector that is less than 1/2 meter; the important thing is that the maximum value of β is less than that presently exists in the machine, so there is little question that one can inject through it.

The question is how to get the beam in and out in this ± 750 in. , i.e. 19 m. Because of the fact that we want to run the proton machine at various energies, and because we would like to keep the machines independent for purposes of filling the machines, I realized that I did not want to put the protons through the electron quadrupoles.

(At 150 GeV, the proton quadrupoles are about 3 kG/in.)
So the first thing to do is to bend the beam. After leaving a ± 5 m space, I put in a long 2 kG magnet to sweep the beams. It is weak to keep the synchrotron radiation down (see Fig. 5). I then put in 2 magnets to put the proton beam back together again. One is 12 kG, the back one is 18 kG. This gives a rather large β . Now that I think about it I'd rather make the β for the electrons larger.

People will probably want to do something with the weak magnet. Note that this magnet bends 40 mrad which is less than is needed for the solenoid polarization scheme.

Now the synchrotron radiation has basically the same emittance pattern as the electrons hence it is focused to a 0.1 - 0.2 mm band. Before you totally give up the idea, think about putting in a dipole as the detector: I think this is a more favorable detector. We do not want to put too much field in there, but the best way to spend your money is to make your field weak and long - that gives you the best lever arm. So why not use a 5 kG dipole in which case we could redo this scheme. We would have to do some thinking about the problem of synchrotron radiation. But the field would be in the right direction to analyze the jets you really want.

So if we had only 0.1 A, we would have a luminosity of 1.5×10^{31} but I can absolutely up, down, right and left guarantee that - today! But what else can we do?

a) Reduce β to 4 m. I use 30 kG/inch in the quad which I think we can get. \mathcal{L} goes to

$$\mathcal{L} = 1.55 \mathcal{L}_0 .$$

b) We can rebunch more. Divide by 7 instead of 3. $1113/7=159$. So we can gain another factor there without changing the electron current, but I am not sure about the stability.

c) I can't gain more by putting more protons in since the emittance goes up. You lose about as fast as you gain. In fact one might think about scraping them and only keeping the good ones.

d) More electron current. It costs rf - say 0.2 A. But I think this is more limited by the number of electrons we can have per bunch. Power at 100 meters radius is 8 MeV/turn, at 150 is $2/3 \times 8$ MeV/turn. One should arrange the polarizing devices so that you can turn it off, and get higher luminosity, since we can increase the current to 0.4 A.

e) I can't do anything to change the total emittances i.e. the product of the emittances in the three planes. But I can trade. I can put in an rf cavity with which I can increase the momentum spread and decrease the emittance of the beam. So if you want I can stretch the interaction region and give you more luminosity. How long is the interaction region - about ± 10 in. So for a ± 20 in. interaction region you get twice the luminosity.

With these things I think you will agree that our luminosity can be something higher than 10^{32} . I will be surprised if we can't get most of that without too much thought.

Q. Would there be any advantage in not bunching the protons?

A. We must bunch the protons because I'm having to separate the beams between the times they meet once and they miss cleanly once. I am not worried about tuneshift - but I am very worried about putting one beam through the edge of another which introduces all sorts of non-linearities.

Q. HERA quotes 2×10^{31} as a luminosity - why can you do so much better?

A. B. Wiik. Everything is different!

Q. What about tuneshift?

A. The beam tuneshifts are small. The energy of my machine is 10 GeV. To increase the electron energy means the weak magnet must get longer - sooner or later we run out of space.

Q. What do you expect the power requirement to be?

A. I would expect to put in about 10 MW of power.

Q. What is the largest radius you can put on the site?

A. I think you could put in just about anything.

I think we should get on and do an ep thing if I could say at this point. For so long I've been pushing it. I meant it when I said I was an old horse thief - except I didn't manage to steal the horse. The way to do it is to get out there and do something. And not to worry too much about the energy. The thing is, you don't get carried away by all these theoretical things that are too often reasons for not doing it. We now look back in the past to the original electron target thing. Because if we'd done that at this point we would not be quibbling. We'd already be trying to figure out how to take the current out of that and into the bigger one and there'd be no argument. The real problem is that you need a laboratory that has both e's and p's at it and real estate. And if we'd once get that then we can up the thing.

Q. Can you move the interaction region to an asymmetric position?

A. Not very easily. The proton machine is an anti-symmetric lattice, so if I move the point with the lowest β in the horizontal you get instabilities.

Q. Is this compatible with $\bar{p}p$?

A. It means effort for the $\bar{p}p$ people.

They don't want their proton bunches colliding with electrons. They depend on long storage times in the doubler.

Q. Would you accelerate the electrons first?

A. I always thought of having the electrons sitting there and then putting 150 GeV protons through and accelerating them.

PROTONS

FIG. 1

β -tron emittance @ 1000 GeV $\cdot 0.2\pi$ mm-mrad. (95%)
 ($n \times 10^{13}$ p $\epsilon = (10n/E) \pi$.) coupled

Synch. $\cdot 2 - \cdot 3$ ev-sec ; - r.f. freq. 53.1 Mc. ($h=1113$)

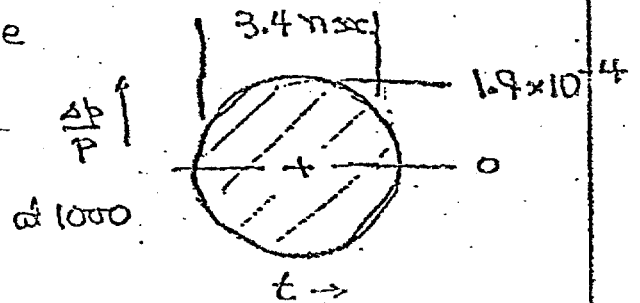
WANT TO REBUNCH INTO EVERY THIRD BUCKET!

a) next collision $3\lambda/2 = 333''$ away.

b) $\dot{n}_p = 6 \times 10^{10}$ / bunch.

c) $\epsilon_p = 0.02\pi$ as before

d) $\epsilon_{\text{synch}} = 1$ ev-sec $\frac{\Delta b}{P}$



ELECTRONS

FIG. 2

HIGHER FREQUENCY \therefore shorter bunch.

Hoe. Betatron emittance - balance between damping and quantum fluctuations.

$$\epsilon \propto \frac{E^2}{\rho} \mathcal{H} \quad \mathcal{H} = \frac{1}{\beta} (\eta^2 + (\beta\eta' + \alpha\eta)^2) \text{ average}$$

ϵ varies as (cell length)³ and can be adjusted in design over a considerable range

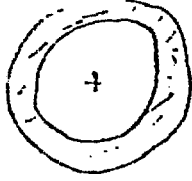
INTENTIONALLY COUPLED TO GET ROUND BEAM

IF $\epsilon = 0.1\pi$ WANT $\beta_e = \beta_p / 5$.

LUMINOSITY - SAME SIZE, ROUND BEAMS

$$\mathcal{L} = \int_{\text{beam}} \text{current in beam 1} \times \text{density in beam 2}$$

$$\sigma^2 = 6\beta/b$$



charge in ring

$$n \cdot \frac{r}{\sigma} e^{-r^2/2\sigma^2} dr$$

density in ring

$$\frac{n}{2\pi\sigma} e^{-r^2/2\sigma^2}$$

$$\mathcal{L} = \frac{b_0}{3} \int_0^{\infty} \underbrace{\frac{n_e r}{\sigma} e^{-r^2/2\sigma^2}}_{\text{electron current}} \cdot \underbrace{\frac{n_p}{2\pi\sigma} e^{-r^2/2\sigma^2}}_{\text{proton density}}$$

Let $I_e = \text{d.c. electron current} = n_e e b_0/3$ $b_0 = 53.1 \text{ Mkh.}$

$$\mathcal{L} = \frac{b_0}{3} \frac{n_p n_e}{4\pi\sigma^2} = \underline{1.51 \times 10^{32} I_e / \beta_p} \quad \text{cm}^2/\text{sec}$$

NOTE. REBUNCHING DID NOT CHANGE THE LUMINOSITY FOR THE SAME n_e BUT IT DID REDUCE THE ELECTRON CURRENT.

$$n_e = 3.52 \times 10^{11} I_e$$

FIG. 3

"LOW" BETA ST. SECTION FOR e-P.

$\beta^* = 5.89 \text{ m.}$ $\alpha^* = 0$ $\eta^* = .48 \text{ m.}$ $\beta_{\text{MAX}} = 237 \text{ m.}$

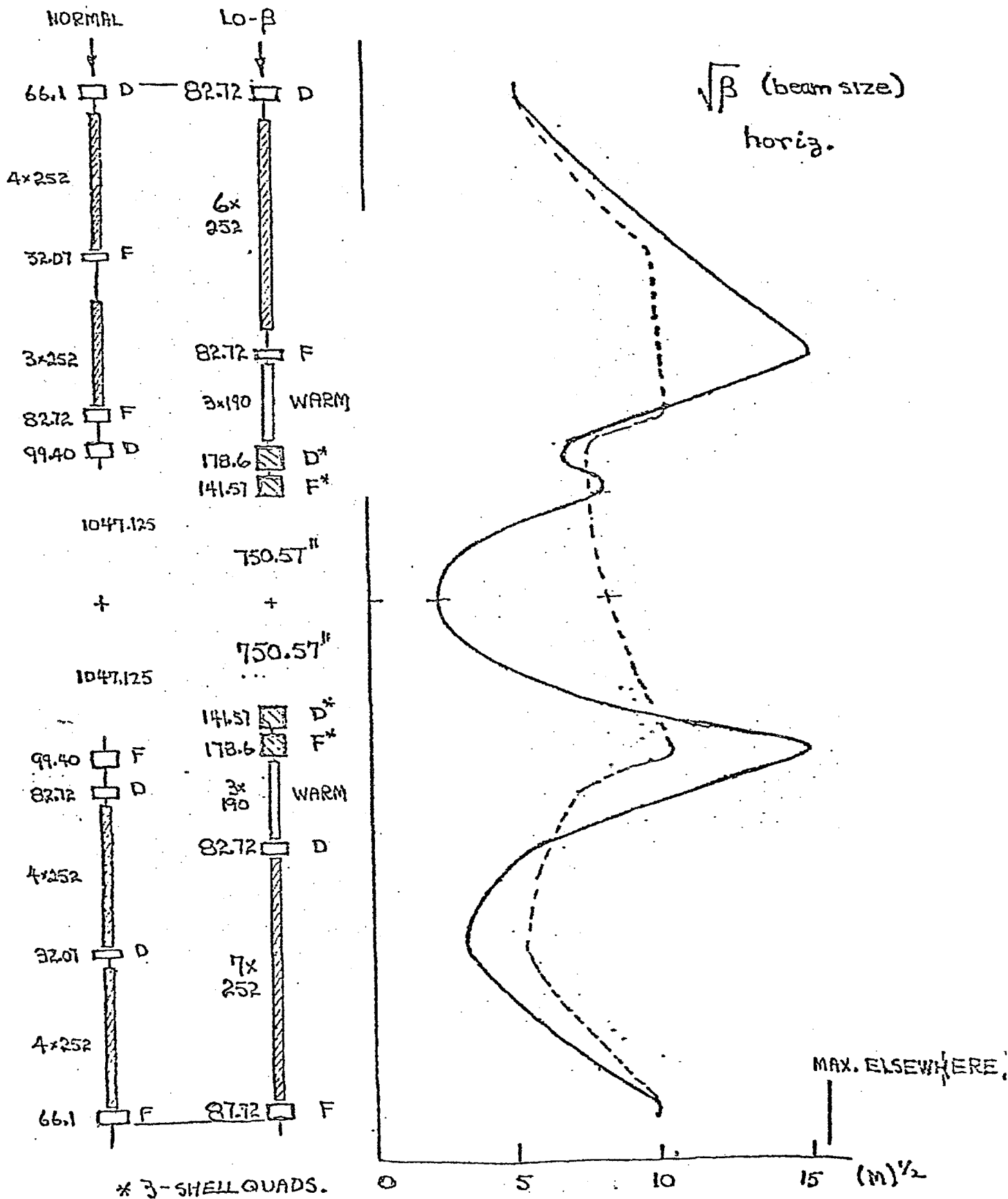
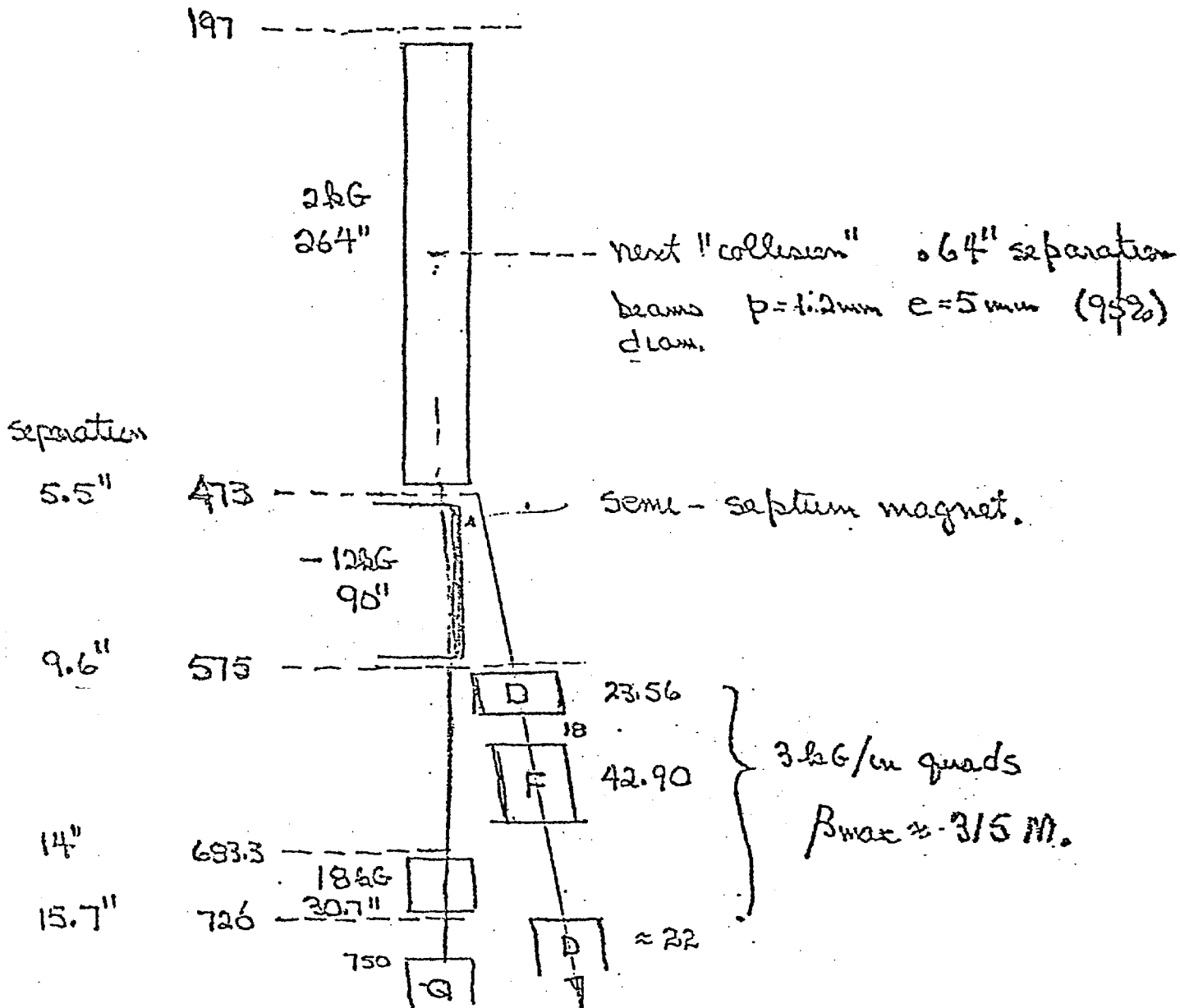


FIG. 4a, b, c

788 MAY 80

$\circ \pm 10'' \quad \bar{I} \quad \beta_p = 232'' \quad \beta_e = 48''$

$\pm 5M$



Possible Interaction Region.

FIG. 5

BASE LUMINOSITY at 0.1 AMPS I_e

$$= 1.5 \times 10^{31}$$

IMPROVEMENTS,

a) REDUCE β_p

3.79 M For $\beta_{max} = 348$ M. uses 30 kG/cm quads

$$L = 1.55 L_0$$

b) Rebunch more - gain as rebunching factor
for same I_e . stability? $\frac{1113}{7} = 159$

c) More protons - slow gain because of
increased emittance.

d) More I_e - costs + b power say 0.2 A.

However - arrange large r.f loss for polarization

so it can be turned off, (use large R)

then increase current to 0.4 A.

e) Space-tracker. Exchange proton E_β
for increased E_{synch} .

Interaction length 0.5 M total \rightarrow 1 M total

$$L = 2 \cdot L_0$$

$$\rightarrow 2 \times 10^{32}$$